Biogeosciences Discuss., 12, 10311–10358, 2015
www.biogeosciences-discuss.net/12/10311/2015/
doi:10.5194/bgd-12-10311-2015

Biogeosciences
Discussions
Open Access

Two-dimensional distribution of living benthic foraminifera in anoxic sediment layers of an estuarine mudflat (Loire Estuary, France)

A. Thibault de Chanvalon[1,2], E. Metzger[1], A. Mouret[1], F. Cesbron[1], J. Knoery[2], E. Rozuel[2], P. Launeau[1], M. P. Nardelli[1], F. J. Jorissen[1], and E. Geslin[1]

[1]Université d'Angers, Université de Nantes, LPG-BIAF, UMR CNRS 6112, 49045 Angers, CEDEX, France
[2]Ifremer, LBCM, Rue de l'Ile d'Yeu, 44300 Nantes, France

Received: 05 June 2015 – Accepted: 17 June 2015 – Published: 08 July 2015

Correspondence to: A. Thibault de Chanvalon (athibaultdc@gmail.com, aubin.thibault-de-chanvalon@univ-nantes.fr)

Published by Copernicus Publications on behalf of the European Geosciences Union.

Abstract

We present a new rapid and accurate protocol to simultaneously sample benthic living foraminifera in two dimensions in a centimeter scale vertical grid and dissolved iron in high resolution (200 µm). Such an approach appears crucial to study foraminiferal ecology in heterogeneous environments. The foraminiferal faunas of the main intertidal mudflat of the Loire estuary are dominated by *Ammonia tepida*, which accounts for 92 % of the living assemblage (CTG-labeled). Its vertical distribution shows a first density maximum at the surface, a sharp decrease in the next two centimeter followed by a well defined second maximum between 3 and 8 cm depth. The heterogeneity of *A. tepida* in this 3–8 cm depth layer was calculated by the Moran's Index and reveals lateral patches with a characteristic length of 1 to 2 cm. We investigate mechanisms potentially responsible for this distribution by observation of burrow structures and two-dimensional high-resolution imaging of dissolved iron. The surface maximum corresponded to the area of maximum oxygen availability. Observable burrows have no clear relation with the distribution of *A. tepida* but were closely related to dissolved iron distribution. Consequently, no evident relation between *A. tepida* and dissolved iron was observed. Nevertheless, two one cm-wide structures, enriched in dissolved iron produced by anaerobic degradation of labile organic matter, corresponded to increased *A. tepida* densities. This observation suggests that within strongly oxygen-depleted sediments, *A. tepida* could still be favoured by labile organic carbon. The main characteristics of the vertical distribution of *A. tepida* are interpreted in the present study as a combination of passive downward transport by biomixing into deeper suboxic (without both oxygen and sulfide) sediment layers and a subsequent mobility driven by a sensitivity to geochemical gradients. We hypothesize that the survival of *A. tepida* in oxygen depleted environments is explained its ability to lower its metabolism between periods of oxygen renewal by bioirrigation.

1 Introduction

Intertidal estuarine mudflats are transitional areas between land and sea. This intermediate position explains the important horizontal, vertical (in the sediment column) and temporal heterogeneities in physical and chemical sediment properties. It also causes heterogeneous ecological niches with scales ranging from micro- to hectometers. When studying such heterogeneous environments, the observational scale has to be chosen in function of the scale of the studied ecological niches variability (Martiny et al., 2006; Morse et al., 2003; Wu et al., 2000). Once this done, it is possible to identify candidate parameters controlling the heterogeneity of the studied niches.

Ecological studies of benthic foraminifera attempt to describe the main factors controlling foraminiferal communities, and their variability on different spatial and temporal scales. The best described pattern concerns their spatial variability in open marine environments, on a hundred-kilometer scale (Jorissen et al., 1995). It shows a regional variability of the spatial organization of foraminiferal taxa in the sediment column, where they occur in a succession of so-called microhabitats. This stratified succession of inhabited sediment layers is supposed to be a response to oxygen and organic matter availability, which change vertically in the uppermost sediment, but also geographically, when going from oligotrophic (deep water, offshore) to eutrophic (shallow water, nearshore) conditions. In estuarine areas, on smaller scales, other controls are invoked (e.g. emersion time, grain size, salinity), but the putative causal relationships between these parameters and the foraminiferal faunas are less well documented. At a kilometric scale, the spatial extent of fresh water mixing seems to be the main process controlling foraminiferal assemblages (Debenay et al., 2006). Nevertheless, hydrodynamics, temporal salinity variations and the frequency of chemical exchanges with the ocean could also be important factors (Debenay and Guillou, 2002). Within the estuary, especially in cross-shore transects, emersion time seems to be a major controlling factor of species distribution at a decametric scale (Berkeley et al., 2007). But others parameters, such as grain size, pH or organic carbon lability could also have a significant impact. Estuarine foraminiferal faunas normally show substantial patchiness at metric scale at the sediment surface (Buzas, 1970). Hohenegger et al. (1989) found positive correlations between species densities and the abundance of "blue-green algae" (non including diatoms), and therefore explained patchiness as a response to food availability. Conversely, Buzas et al. (2002), on the basis of spatial and temporal data of subtidal assemblages, argue that benthic foraminiferal heterogeneity is resulting from pulselike responses (localized short and strong density maxima followed by a return to background conditions) to unknown parameters. At a decimeter scale, the rare studies performed on intertidal mudflats highlight that grain size and topography could be important controls (Lynts, 1966; Morvan et al., 2006). Finally, according to our knowledge only three publications have analyzed the spatial surface organization at a centimeter scale, using an adequate sampling grid (Buzas, 1968 in Rehoboth Bay, Delaware; de Nooijer, 2007 in the Wadden Sea and Olsson and Eriksson, 1974, in the Swedish coast). These three studies show that foraminiferal densities present a patchy distribution. Buzas (1968) hypothesized that this could be due to reproduction, leading to very localized intermittent density maxima. Another field approach, at a centimeter scale, is to sample around inhabited burrows, using a non regular sampling scale, by defining position, size and shape of each sample according to the burrow shape. In this way Aller and Aller (1986) and Thomsen and Altenbach (1993) studied the foraminiferal distribution around macrofaunal burrows at subtidal stations and observed a threefold enrichment of foraminiferal density in the burrow walls. With a similar sampling strategy, Koller et al. (2006) showed a three hundred-fold enrichment of foraminiferal densities in the burrow walls of an intertidal station. These studies highlight the importance of macrofaunal activity as a potential control of meiofaunal spatial organization. They suggest the presence of oxic microenvironments around the burrows generated by bio-irrigation, attractive because of organic matter enrichment (Aller and Aller, 1986). Foraminifera could specifically colonize these environments favorable for aerobic respiration. Unfortunately, the sampling strategies used in these studies did not allow the comparison of the foraminiferal micro-distribution with other controlling factors (physico-chemical environmental parameters) or mechanisms (functional response of foraminifera) likely to cause foraminiferal heterogeneity. Thus, the increased density observed in burrow walls (mostly at a millimeter scale) was not compared to a "background heterogeneity" at the same scale. Unfortunately when the density increase of the foraminiferal faunas is not at least one order of magnitude (expected background heterogeneity scale) it is necessary to do so, before the importance of burrow walls, compared to others factor, can be assessed.

Factors causing heterogeneity at a submeter scale in intertidal mudflats are firstly due to the heterogeneity of the sedimentary deposits: e.g., grain size, chemical composition of mineral grains and terrigenous organic matter content. Once settled, particles are subject to chemical reactions and benthic faunal activity, both creating sediment column heterogeneity. Main factors of heterogenic transformations reported in the literature include: presence of microorganisms stratified in function of their metabolism, occurrence of biomixing and/or bioirrigating macrofauna, presence of decaying dead organisms, fecal pellets, authigenic organic matter from microphytobenthos and authigenic mineral precipitation (Aller and Aller, 1986; Chandler, 1989; Findlay, 1981; Hebert et al., 2007; Lewandowski et al., 2002; Lewandowski and Hupfer, 2005). Many of these factors impact pore water geochemistry, which can therefore be used as an indicator of their occurrence. The recent development of pore water sampling techniques with high resolution in two dimensions offers the advantage of providing simultaneously information on vertical and horizontal scales. These methods allow the description of the high heterogeneity below a decimeter scale, and specifically to address lateral heterogeneity, that can be important in intertidal sediments (Santner et al., 2015; Stockdale et al., 2009). As foraminiferal densities should reflect the heterogeneity of their controlling factors, a sampling of environmental factors taking into account lateral heterogeneity should yield more precise information about the mechanisms controlling foraminiferal communities. Previous studies at this scale (Aller and Aller, 1986; Buzas, 1968; Koller et al., 2006; de Nooijer, 2007; Olsson and Eriksson, 1974; Thomsen and Altenbach, 1993) did not analyze pore water chemistry, which could have been very helpful to explain foraminiferal heterogeneity. In order to fill this gap, we developed a new sampling technique allowing both visual analysis of sedimentary features and burrowing activity, quantification of living foraminiferal assemblages at a centimeter scale, in two dimensions, and chemical analyses of pore water dissolved species (Fe^{2+} and dissolved reactive phosphorus (DRP)) at a submillimeter scale. Our methodology is efficient, robust, and allows the simultaneous description of spatial heterogeneity of all parameters at a centimetric scale. The nature of the obtained dataset allowed us to investigate, for the first time, the putative relationships between benthic foraminiferal assemblages, dissolved chemical distribution and macrofaunal burrowing structures.

Aerobic metabolism is supposed to be the dominant metabolic pathway applied by foraminifera, which implies that the presence of both labile organic carbon and oxygen is a prerequisite for foraminiferal prosperity. Nevertheless, living foraminifera are commonly found in anoxic sediment (Richter, 1961), especially in intertidal environments. Recently, several studies have focused on alternative metabolic mechanisms that can explain the occurrence of living foraminifera in anoxic environments. Some of these mechanisms can explain long term survival in anoxia: anaerobic respiration such as denitrification (Risgaard-Petersen et al., 2006) and endo and/or ectobiosis (Bernhard et al., 2012). Other mechanisms allow organisms to survive in hypoxia or transient anoxia: microaerophily (Leutenegger and Hansen, 1979), dormancy (Bernhard and Alve, 1996), and distant aerobic respiration through pseudopodia (Bernhard and Alve, 1996). These putative response mechanisms can lead to contrasted conclusions concerning ecological strategies. For example, a high density of living foraminifera in burrow walls compared to anoxic surrounding sediments may be explained by a positive response of the foraminiferal community to the availability of oxygen and labile organic matter (Aller and Aller, 1986; Loubere et al., 2011) or as the involuntary consequence of passive downward transport due to macrofaunal bioturbation (Alve and Bernhard, 1995; Moodley et al., 1998). These different interpretations will be evaluated on the basis of a data set obtained from an intertidal mudflat with a high density of benthic foraminifera and an important macrofaunal community. We will confront all combinations of putative mechanisms listed above with the data obtained with our novel approach to finally present a coherent conceptual model for the the distribution of foraminiferal assemblages.

2 Material and methods

2.1 Site description

The Loire estuary (NW coast of France) is hyper-synchronous: it shows an increasing tidal range upstream (Le Floch, 1961) reaching a maximum-spring-tidal range of about 7 m at 40 km from the mouth. At Donges (in the high tidal range area, right shore) the daily salinity range is about 20. Seasonally, salinity fluctuates from 0 during floods to 30 during low-water periods (network SYVEL, GIP Loire Estuaire). On the opposite shore, the largest mudflat of the estuary ("Les Brillantes", ~ 1350 ha, Fig. 1) extends downstream from the city of Paimboeuf. During high tide, hydrodynamics (tide, wind induced waves, flow) constrains the sediment deposition/resuspension cycle whereas during low tide, biological factors (bioturbation, biofilm stabilization, benthic primary production) become more important and generate sediment burial and chemical transformations. Microphytobenthic biofilms vary annually between 20 $mg\,m^{-2}$ in January and 60 $mg\,m^{-2}$ in July (Benyoucef et al., 2014). Our sampling site (47°16′56.00′′ N, 2°3′47.00′′ W) is located on the slikke, below the Mean High Water Neap Tide level (MHWNT), about 20 m offshore from an active one meter high eroded cliff. Sediment is mainly composed of silt (92 %) with some clay (6 %) and sand (2 %) (Benyoucef, 2014).

We sampled in the first half of May 2013, two weeks after a major flood (discharge volume at Paimboeuf > 2500 $m^3\,s^{-1}$, hydro.eaufrance.fr). During sampling the river discharge was 835 $m^3\,s^{-1}$ on average. Air temperature was 12.7 °C, the weather was cloudy and salinity in the surface waters of the main channel ranged from 0.6 to 20 (data from SYVEL network). Sediment samples were collected at the beginning of low tide. In the first centimeter of the sediment column, salinity was 5.57 ± 0.5 (data not shown). Porosity decreased from 0.917 to 0.825 in the first 5 cm (data not shown). The calcite saturation state, calculated from alkalinity, sodium, calcium concentrations and pH (Boudreau, 1996; Hofmann et al., 2010; Millero, 1979, 1995; Mucci, 1983; Mucci et al., 2000) was above 1.0 until 9 cm depth (data not shown). The macrofauna was mainly composed of *Hediste diversicolor* (630 ind m^{-2}) and *Scrobicularia plana* (70 ind m^{-2}) (I. Métais, personal communication, 2015).

2.2 1-D sampling and processing

Three cylindrical cores (diameter 8.2 cm) were sampled using Plexiglas tubes. The first core was dedicated to foraminiferal analysis and was sliced immediately after sampling, every two millimeters (10.6 cm^3 of sediment) from 0 to 2 cm and every half centimeter (26.4 cm^3 of sediment) between 2 and 5 cm. Within one hour after retrieval, in order to distinguish living foraminifera, sediments were incubated with CellTracker™ Green at a final concentration of 1 µmol L^{-1} in 50 mL of estuarine water for 10–19 h (Bernhard et al., 2006). CellTracker Green is a non fluorescent molecule, which is hydrolyzed by nonspecific esterases, producing a fluorescent compound. After incubation, samples were fixed in 3.8 % Borax-buffered formalin and stored until analysis. In the laboratory, samples were sieved over 315, 150, 125 and 63 µm meshes, and the 150–315 µm fraction was examined using an epifluorescence stereomicroscope (i.e., 485 nm excitation, 520 nm emission; Olympus ZX12 with a fluorescent light source Olympus URFLT or Nikon SMZ 1500 with a PRIOR Lumen 200). All foraminifera that fluoresced continuously and brightly were wet picked, air dried, identified and counted.

The two other cores were used to constrain geochemistry. The first core was dedicated to solid phase geochemistry and microelectrode profiling. The solid phase was characterized by total organic carbon and reactive iron, manganese and phosphorus, extracted by an ascorbate reagent (buffered at pH 8) during 24 h (Anschutz et al., 1998, 2005; Hyacinthe et al., 2001; Hyacinthe and Van Cappellen, 2004; Kostka and Luther III, 1995). See more details in the Supplement (Sect. S2). Oxygen was analysed with

Clark's type electrodes (50 µm tip diameter, Unisense©, Denmark). In the second core, Diffusive Equilibrium in Thin film in one dimension probes (DET-1D, adapted from Davison and Zhang, 1994; Krom et al., 1994) were incubated during one night for dissolved iron, manganese and phosphorus. Gel samples were eluted in HNO_3 0.01 M and analyzed by ICP-AES. See more details in the Supplement (Sect. S6.2).

2.3 2-D sampling and processing

To sample simultaneously pore water and sediment, we used a "jaw device", composed of two main parts (jaws). The first jaw is an unconstrained DET gel probe, which samples the dissolved chemical species from the pore water at high resolution, whereas the second jaw samples a 2 cm-thick sediment slice, in which we sub-sampled 1 cm^3 aliquots for foraminiferal analysis. Figure 2 shows the sampling outlay: deployed in the sediment at low tide, the first jaw is a 250 mm × 200 mm × 2 mm polycarbonate (Poly-methyl methacrylate) plate with a central depression of 1 mm that holds a 2-D gel probe. The probe is made of two layers: (1) a 180 mm × 97 mm × 0.92 mm polyacrylamide thin-film prepared and rinsed with Milli-Q (Krom et al., 1994) which reaches equilibrium in a few hours once incubated (called "DET-2D gel") and (2) a PVDF porous (0.2 µm) membrane to protect and maintain the gel and control diffusion. The DET-2D gel was prepared and mounted less than one week before sampling, conserved in a wet clean plastic bag and was deaerated by N_2 bubbling for about 6 h before deployment. On both lateral sides of the central depression (Fig. 2), plastic rails (2 cm high) were fixed in order to guide the second jaw to slide along the plate. The second jaw is a stainless steel plate (1.5 mm thick) bent on both sides. After equilibration (5 h) of the 2-D gel, the second jaw was inserted along the guides of the first jaw and the whole was gently pulled out of the sediment. Once on shore the 2-D gel was separated from the sediment, covered with a plastic-coated aluminum plate and stored in an icebox with dry ice pellets (Cesbron et al., 2014), until final storage in a freezer (–18 °C). The system allows sampling a parallelepiped of sediment (2 cm thick) of which one side faces the 2-D gel probe.

The sediment plate was manually cut (with stainless steel trowels) within 30 min (Fig. 3b) in 1 cm^3 cubes for a surface of 10 cm × 8 cm (width × length). Figure 3 compare 1-D and 2-D sampling of foraminifera. Next, these sediment cubes were labeled with CTG to recognize living foraminifera (as for the core slices, see Sect. 2.2). Considering an error of 1 mm for each cut, the volume uncertainty was $\sim 14\,\%$, except for surface samples where the microtopography of the sediment surface considerably increases volume uncertainty.

The DET-2D probe was analyzed in order to obtain the concentrations of dissolved iron and dissolved reactive phosphate (DRP) (Cesbron et al., 2014). Quickly, after thawing at ambient temperature, the sample gel was recovered by a reactive gel equilibrated in specific colorimetric reagents. Fifteen minutes after contact, a picture (reflectance analysis) of superposed gels was taken with a hyperspectral camera (HySpex VNIR 1600) and analyzed (see 6.3 for more details). The resolution (surface area of pixels) was 211 µm × 216 µm. The estimated incertitude is 10 % for iron and 11 % for DRP. See more details in the Supplement (Sect. S3). To compare the geochemical species distribution (at submillimeter resolution) and foraminiferal density (at centimeter resolution), a handmade *R* code was written allowing the downscaling of chemical resolution from 0.2 mm to 1 cm.

2.4 Statistical analyses

Patchiness effect or autocorrelation, interpreted as the fact that a density of one square depends on its neighbors, was explored using spatial correlograms built using Moran's Index (I), computed with *R* (package "spdep" following (Bivand et al., 2008; Borcard et al., 2011; Fortin and Dale, 2005; Legendre and Fortin, 2010), Eq. 1). This index was applied to benthic meiofauna by Blanchard (1990) and Eckman and Thistle (1988) and to foraminifera by Hohenegger et al. (1993). This Index calculates the similarity of pair values for one neighborhood, a neighborhood being defined by a weight ($w_{i,j}$) function of the distance (d) between pairs.

$$I(d) = \frac{\sum_{i,j}^{n} w_{i,j}(d)\left(x_i - \overline{x}\right)\left(x_j - \overline{x}\right)}{\sqrt{\sum_{i}^{n}\left(x_i - \overline{x}\right)^2}} \times \frac{n}{\sum_{i,j}^{n} w_{i,j}(d)} \tag{1}$$

Here, the neighborhood is restricted to sediment cubes in direct contact (4 neighbors per sample with a weight of 1, others have 0, also known as “rook connectivity”, Fortin and Dale, 2005). With this configuration, Moran’s Index is −1 for a contrasted organization (perfect negative correlation between neighbors) and +1 in case of grouped organization (perfect positive correlation between neighbors). A value of $I = 0$ corresponds to no organization or random distribution. The correlogram plots Moran’s Index vs. the order of the neighbors (o.n.). A decrease of the Moran’s Index from positive to negative values characterizes a patchy distribution. The characteristic length of the patchiness is defined as the order of neighbors when $I_{\text{o.n.}} = 0$ (Legendre and Fortin, 1989). Two dimensional non-random organization has been tested with the alternative hypothesis $I_{\text{o.n.}} > I_0$ where I_0 is determined with a Monte-Carlo method. The second test examines if there is a preferential direction in the organization (isotropy). Again, the alternative hypothesis $I_{\text{o.n.}} > I_0$ for Moran’s Index is used, restricting the distance to the tested dimension (vertical or horizontal). Thus, in our case, each sample was compared only with its lateral or vertical neighbors (i.e., 2 neighbors per test).

3 Results

3.1 Visual features on the sediment plate

The sediment slice obtained from the “jaw device” shows different sedimentary features (Fig. 4a). The picture presents the sediment facing the DET-2D gel. When they are parallel to the cutting plan, burrows are visible over their entire length (e.g. Fig. 4a arrow “a”). When they are perpendicular to the cutting plan, they appear as a dark hole (Fig. 4a arrow ‘b’). Our visual observations are summarized in Fig. 4b. Eight burrows were observed to be connected to the sediment surface (Fig. 4a number 1 to 8); their traces mostly extended vertically to deeper layers. Only one of these burrows appeared to extend below 10 cm depth, others stopped or could eventually continue in another, not visible plan. Below 10 cm depth, the burrow density was decreasing until 15 cm depth, where burrows were rarely observed and the sediment was dark (Fig. 4a). During slicing of the sediment, in some of the burrows (about 3 mm diameter) living polychaetes (*Hediste diversicolor*) were observed.

3.2 Living foraminiferal distribution

Figure 5 shows the distribution of CTG-labelled foraminiferal density determined in an entire sediment core (Fig. 5a) and in the sediment plate described above (Fig. 5b). In the sediment core, *Ammonia tepida* was by far the dominant species, accounting for 92 % of the total assemblage. The second most frequent species, *Haynesina germanica*, represented almost 8 %. The vertical distribution of *A. tepida* in the sediment core presents a three step profile: high densities (above 15 ind cm^{-3}) in the 6 first millimeters, a rapid decrease to minimal densities of about 5 ind cm^{-3} around 1.0 cm, followed by a progressive, somewhat irregular increase until 7–10 ind cm^{-3} below 2 cm depth. The sediment plate (Fig. 5b) shows the CTG labelled *A. tepida* density in two dimensions. In the plate, *A. tepida* represented more than 93 % of the assemblage. In the 64 samples of 1 cm^3, densities of *A. tepida* ranged from 0 to 38 ind cm^{-3}. Also in the sediment slice, living *A. tepida* densities showed a clear three step pattern, with high densities at the surface (13 to 38 ind cm^{-3}), lower density between 1 and 3 cm depth (0 to 24 ind cm^{-3}) and increasing values below (7 to 31 ind cm^{-3}). The richest samples ($\geq$ 27 ind cm^{-3}) were found in the topmost cm and below 6 cm depth. The poorest samples ($\leq$ 5 ind cm^{-3}) were found between 1 and 3 cm depth. However, the *A. tepida* densities on the plate showed also substantial lateral variability. For example, in the first centimeter, *Ammonia* density ranged between 13 and 38 ind cm^{-3}, and in the level below from 0 to 12 ind cm^{-3}.

3.3 1-D geochemical features

Figure 6 shows both solid and dissolved chemical species obtained from a core sampled next to the core dedicated to foraminifera. Total organic carbon (C_{org}, black circles, Fig. 6a) decreased from 2700 to 1900 µmol g(dry sed)$^{-1}$ in the first centimeter, then increased sharply until 1.5 cm depth, and finally decreased progressively from 2700 to 2400 µmol g(dry sed)$^{-1}$ at 5 cm depth. Figure 6a and b shows the vertical distribution of dissolved oxygen. The three profiles that are shown (out of 18) are considered representative of the lateral sediment heterogeneity. Most of the oxygen concentration profiles show the exponential trend typical for undisturbed marine sediments (2 profiles in Fig. 6b, with light grey and white diamonds) (Berg et al., 1998; Revsbech et al., 1980). However, one third of the O_2 profiles diverged from the exponential model, showing an interruption of the decreasing trend, or even a local increase, at depth (e.g. the profile with dark grey diamonds represented in Fig. 6b). The Oxygen Penetration Depth (OPD) remained relatively constant around 2.0 mm (SD = 0.2 mm, $n = 18$) despite this heterogeneity.

Figure 6c–e shows the distribution of manganese, iron and phosphorus, respectively, both in the dissolved phase (grey and open diamonds) and in the easily reducible solid phases (black circles, extracted by ascorbate leaching, Anschutz et al., 2005; Hyacinthe et al., 2006). Extracted manganese (mainly (hydr)oxide, black circles in Fig. 6c) showed a strong enrichment of the easily reducible solid phase (until 13 µmol g(dry sed)$^{-1}$) in the first two millimeters, where an important upward diminution was visible in both replicates of the dissolved phase (grey and open diamonds in Fig. 6c). Below, the solid phase showed a slightly decrease from 7.9 to 5.6 µmol g(dry sed)$^{-1}$ until 5 cm depth. The dissolved manganese concentration decreased between 4 and 9 cm depth in both replicates (from 70 to 30 µmol L^{-1}). In the solid phase, iron, phosphorus and manganese are strongly correlated when the surface sample is not considered ($r^2 = 0.70$ and 0.55 between iron and manganese, and iron and phosphorus, respectively). Profiles of dissolved iron and phosphorus are also strongly correlated ($r^2 = 0.90$, slope = 1.87 and $r^2 = 0.47$, slope = 1.31 for replicates A and B). Iron and phosphorus were remobilized, and therefore appeared in the dissolved phase, between 1 and 9 cm. Both replicates of dissolved iron showed the same four well described maxima (at least six samples for each maximum) at 2.3, 3.3, 5.9 and 7.3 cm depth but with different concentrations. In replicate A (open diamonds) these maxima had five times higher iron concentrations (up to 700 μmol L^{-1}) than in replicate B.

3.4 DET-2D gel

Figure 7 shows the 2-dimensional distribution of dissolved iron and phosphorus obtained from the gel probe mounted on the first jaw. Figure 7a shows a picture of the gel after equilibration with the colorimetric reagents (pink coloration corresponds to iron and blue to dissolved reactive phosphorus (DRP)). In order to study the relationship between the distribution of dissolved species and sedimentary features, the visual interpretation of the picture (Fig. 4b) is shown again in Fig. 7b. Figure 7c and d represents separate mappings of dissolved iron and DRP in an arbitrary concentration color scale. In order to facilitate the description, the figures were subdivided in centimetric squares labeled with letters for the horizontal position and numbers for the vertical position. Dissolved iron and phosphorus both appeared a few millimeters below the sediment water interface. They are positively correlated for the whole plate ($r^2 = 0.59$, slope = 2.7). Despite their patchy distribution, both species can be observed along the entire length of the gel probe (i.e. 17 cm depth). A main feature was the occurrence of two prominent vertical structures enriched in dissolved iron and in DRP (A–B/6–9 and F–G/5–14). The highest concentrations, of about 170 and 50 μmol L^{-1} for iron and phosphorus, respectively, were found in the right structure, in the squares F8–9. In the left structure, iron and phosphorus maxima were around 120 and 25 μmol L^{-1}, respectively.

The visual interpretation (Fig. 7b) suggests a relationship between dissolved chemical species and bioturbation. Some burrows seem to correspond to a drastic decrease or disappearance of dissolved species (e.g. burrow numbers 2, 4, 6 (until 5 cm depth) and 8 in deeper part of the sediment), whereas other burrows seem to correspond to an iron enrichment (F–G/5–9). However, centimetric patches in A–B/6–9, H8 and F–G17 seem to be unrelated to burrow structures. Below 10 cm depth, the sediment was dark and iron globally decreased whereas DRP increased.

4 Discussion

4.1 A methodological improvement to characterize sediment heterogeneity

Here, we present for the first time a methodology allowing to study simultaneously the vertical and horizontal heterogeneity of chemical species and living foraminifera (determined by CTG staining) in the first centimeters of the sediment. The method was tested on a tidal mudflat of the Loire estuary. The investigated sediment is characterized by a very shallow oxygen penetration depth of 2 mm, and contrasted conditions deeper down. Heterogeneity is quantified in the suboxic part of the sediment (without both oxygen and sulfide, Aller, 2014). Such a simultaneous study of geochemistry and the living foraminiferal community is possible by using a simple and cheap sampling tool, “the jaw device” (not commercially available), which is easy to use in intertidal areas and may be adapted for deeper environments. In practice, the analyses of the living foraminifera in the 64 samples of the sediment slice did not take more time than the analysis of an entire core (until 5 cm) and yielded important information about infaunal spatial patchiness.

Figure 8a compares the vertical density distribution of *A. tepida* between the core (dark triangles) and the jaw device (whisker plots), sampled a few decimeters apart. Despite the different vertical sampling resolution, the densities observed in the core are in agreement with the average densities observed in the sediment slice samples (sampled with the “jaw device”). This similarity suggests a limited horizontal heterogeneity of *A. tepida* at a decimetric scale, although it is impossible to draw firm conclusions on the basis of only two samples (the core and the jaw device). Dissolved iron shows a different behavior. Figure 8b compares replicates of one night incubation DET-1D (full and open triangles) with the 1-D equivalents of the DET-2D. These equivalents correspond to the horizontal mean of 2 cm wide columns extracted from the high resolution dataset (Fig. 7c). From the four 1-D equivalents obtained, the extremes and the mean are represented in the Fig. 8b. The 1-D equivalents differ from the DET-1D pattern, because the gradients are less abrupt, and there is no important decrease below 6 cm depth. The contrast between the two sampling devices can be due to a high heterogeneity at a decimetric scale of dissolved iron or to the differences between the two methodologies (different incubation time, in situ/ex situ).

The plate (2-D) method yields additional information about horizontal distribution. Figure 9 shows the Moran’s Index correlograms applied between 3 and 8 cm depth where the living foraminiferal density is high despite the lack of oxygen. This index allows to quantify the heterogeneity and to determine a characteristic length of the patchiness. Figure 9a shows that the spatial organization of *A. tepida* is patchy at a centimeter scale ($I_1 = 0.24$, p value = 0.013). For farther neighbors the Moran’s Index values drop to zero, describing a random organization. Concerning vertical and horizontal heterogeneities, Moran’s index values for direct neighbors are 0.02 and 0.47, with p values of 0.38 and 0.001, respectively. For second order neighbors, values do not significantly differ from 0 in either direction (data not shown). This means that *A. tepida* specimens tend to be grouped in horizontal spots with a characteristic length of 1 to 2 cm. Figure 9b shows the Moran’s Index correlogram for iron at 1 cm scale resolution (DRP is similar and not shown). It shows strong patchiness ($I_1 = 0.7$) for direct neighbors in either direction, with a characteristic length of 3–4 cm. Thus *A. tepida* (Fig. 9a) and dissolved iron (Fig. 9b) patches have different characteristic lengths. This suggests that different mechanisms control these parameters, in spite of the fact they are necessarily affected by the same environmental factors. This is an unexpected result, since most conceptual models explain benthic foraminiferal distribution in the sediment as a direct response to geochemical gradients (e.g. Fontanier et al., 2002; Jorissen et al., 1998; Langezaal et al., 2006; Langlet et al., 2013; Van der Zwaan et al., 1999) and dissolved iron is intimately coupled with other geochemical gradients. This paradox can be solved by better understanding the factors likely to generate chemical heterogeneity in two dimensions, and by relying these factors to the foraminiferal lateral and vertical distribution.

4.2 Factors generating chemical heterogeneity

The heterogeneity of geochemical patterns is mainly explained by the availability of oxidants mineralizing organic carbon (Terminal Electron Acceptor Process (TEAP), Froelich et al., 1979). Figure 6 shows coherent results with TEAP: oxygen is rapidly consumed by respiration (about 2 mm depth, Fig. 6b); next, reduced dissolved manganese appears (Fig. 6c). Dissolved iron appears still deeper, with a first maximum at 2 cm depth. The slopes of the concentration profiles are steeper and the reactive solid phase (Fig. 6d and c) is more concentrated for iron than for manganese, suggesting a higher reactivity. The theoretical horizontal invariance suggested by the TEAP model proves defective in our suboxic layers, as shown by the multiple maxima of iron in Fig. 6d and the high lateral heterogeneity observed in Fig. 7a and c. This suggests that a strictly vertical stratification of redox zones, defining a similar foraminiferal microhabitat succession, is not a reasonable assumption. Since dissolved iron is very reactive and spread over a wide depth interval at our site, it is a good candidate to trace the factors generating lateral heterogeneity.

4.2.1 Macrofaunal impact on heterogeneity

Macrofauna is assumed to be the most important cause of sediment heterogeneity at a scale of 0.01 cm (roughly the foraminiferal scale) to 100 cm (station scale) because of its ability to move objects. In this way, macrofauna determines whether other factors

Title Page
Abstract Introduction
Conclusions References
Tables Figures
◀◀ ▶▶
◀ ▶
Back Close
Full Screen / Esc
Printer-friendly Version
Interactive Discussion

can impact the heterogeneity of dissolved iron and/or *A. tepida*. Macrofauna modifies: (i) the sediment texture/composition (burrow walls or fecal pellets), (ii) the redox conditions, by ventilation of their burrows with oxygenated water (bioirrigation) and (iii) particle arrangement by crawling or burrowing (biomixing) (Meysman et al., 2006). The latter two mechanisms are regrouped under the term bioturbation (Kristensen et al., 2012). The efficiency of biomixing mechanisms to homogenize other factors mainly depends on two aspects (see Meysman et al., 2010a; Wheatcroft et al., 1990 for a more detailed discussion). Firstly, the biomixing species assemblage: at the "Les Brillantes" mudflat, the main macrofaunal species are *Hediste diversicolor* (630 ind m^{-2}) and *Scrobicularia plana* (70 ind m^{-2}, I. Métais, personal communication, 2015). *H. diversicolor* is a gallery-diffusor (particle mixing due to burrowing activity) whereas *S. plana* is an epifaunal biodiffusor (particles mixing in a random way over short distances along the surface, e.g., François et al., 2002; Kristensen et al., 2012). These species generate homogeneity (i.e. can be described by diffusive model) according to the second criterion: the relation between the average time of existence of the studied objects in the reworked area and the average time between two bioturbation events. Frequent (relatively to the time of existence of the studied objects) bioturbation events generate homogeneity whereas rare bioturbation events generate heterogeneity.

Figure 10 compares the time of existence of different objects in the sediment column between 3 and 8 cm depth with the waiting time between reworking events. Both heterogeneity or homogeneity can be generated depending of this two factors. According to Meysman et al. (2003, 2008) the waiting time between reworking events is days to months depending on macrofaunal density and diversity. For our site, which is strongly bioturbated, we suggest a waiting time of about 1 month, in agreement (or above) with values from *H. diversicolor* models (Duport et al., 2006; François et al., 2002; Gillet et al., 2012; Schiffers et al., 2011). Taking into account a mean sedimentation rate below 1 cm yr^{-1}, amorphous (non reactive) grains have a time of existence superior to 5 years. This is two orders of magnitude more than the waiting time between reworking events, enough to consider that amorphous grains are homogenized. This homogenization may be described by a diffusive model. The mean time of existence of *A. tepida* between 3 and 8 cm depth is evaluated to be roughly one year (Langlet et al., 2013; Nardelli et al., 2014). Thus, on average, each *A. tepida* individual is transported more than ten times during its lifetime by biomixing events, enough to represent the homogenization of the *A. tepida* population by a diffusive model. This is in agreement with the absence of correspondence between visible burrows (Fig. 4b) and foraminiferal densities (Fig. 5b). On the contrary, oxygen supplied by burrow ventilation events have an existence of less than a few hours after each bioirrigation event (Fenchel, 1996; Wenzhofer and Glud, 2004) and recently burrowed authigenic precipitation and authigenic organic matter, fecal pellets and burrow walls have a time of existence of a few weeks (Alldredge and Cohen, 1987; Zhu et al., 2006). Consequently, these factors are not homogenized by biomixing. In conclusion, biogenic factors, defined as biogenic particles (decaying macrofauna, fecal pellets, burrow walls, authigenic organic matter), active burrows supporting bioirrigation and biomixing seem to be the only factors capable to generate heterogeneity on a submetric scale on “Les Brillantes” mudflat. This implies that these are the only factors able to generate heterogeneity of dissolved iron and *A. tepida*.

4.2.2 Geochemical impact of biogenic factors

The biogenic factors discussed in the previous section cause either an increase of labile carbon availability (biogenic particles) or an increase of oxidant availability (active burrows supporting bioirrigation and biomixing, Aller and Aller, 1986, Aller, 2004; Arndt et al., 2013). Dissolved iron shows two opposite types of behavior (Aller, 1982): (1) iron precipitates as a hydroxide when the oxidative state of the pore water surrounding active burrows increases (MB Meyers, 1987; Meysman et al., 2010b; Zorn et al., 2006). This is confirmed by visible burrows in Fig. 7b in which both dissolved iron and DRP are depleted (Fig. 7c and d, numbers 2, 4, 6 (above 6 cm depth) and 8 and burrows in B–C–D13, E9–11 and A–B9). These structures are mainly vertical and have a length often exceeding 3 cm; in agreement with the Moran’s Index correlogram. Conversely, the long burrow F–G/5–9, enriched in dissolved iron is considered abandoned, because of the absence of oxygen renewal. This feature was also observed for some burrows by Cesbron et al. (2014) and Zhu and Aller (2012). (2) Iron is released by anaerobic respiration where biogenic particles increase labile carbon availability, and thereby decrease the oxidative state of surrounding pore waters (Robertson et al., 2009; Stockdale et al., 2010). The geometry and isolation from visible burrows of patches A/7–8, G–H/8–9 and F–G17 in Fig. 7c and d suggest that they could represent centimeter-wide labile organic matter patches. Summarizing, the two identified sources of heterogeneity can be identified by the opposite dissolved iron gradients and a different characteristic length of iron patches.

4.3 Mechanisms controlling the *A. tepida* distribution

The Fig. 5a clearly describes a three-step pattern in the distribution of *A. tepida*, with high densities at the surface, low densities between 1 and 3 cm depth and a somewhat surprising increase below. This pattern was reported, but not discussed, from a few replicates from Alve and Murray (2001) and Bouchet et al. (2009) in intertidal environments. In our study, the 8 vertical replicates from the plate sampling confirm the robustness of this pattern. The question is what mechanisms are able to explain our observation of a high density between 3 and 8 cm depth, and an organization in centimeter-wide patches.

4.3.1 Foraminiferal metabolism

Generally, aerobic metabolism is considered as the dominant mechanism in oxic conditions since it is energetically most efficient. In fact, Figs. 5a and 8a clearly describe maximal densities of *A. tepida* at the sediment surface (0–2 mm depth) and low densities below (6–18 mm depth). This strong gradient highlights the presence of a continuously oxygenated microhabitat close to the sediment–water interface, favorable for *A. tepida*. Energetic considerations and some observations that report a strong seasonal variability in the oxic zone (Barmawidjaja et al., 1992; Moodley, 1990), lead Berkeley et al. (2007) and De Stigter et al. (1999) to assume that foraminifera reproduce preferentially in the oxic layer. The resulting profile from superficial reproduction is represented in Fig. 11. However, this hypothesis cannot explain the unexpected high density between 3 and 8 cm depth.

Since the work of Richter, (1961), numerous publications (Bernhard and Sen Gupta, 2003; Jorissen et al., 1992; Moodley and Hess, 1992) have reported living benthic foraminifera in suboxic sediment layers. Several in situ (Bouchet et al., 2009; Goldstein et al., 1995) and laboratory studies (Moodley et al., 1998; Moodley and Hess, 1992; Nardelli et al., 2014; Nomaki et al., 2014; Pucci et al., 2009) with *A. tepida* also reported survival, activity and even calcification in suboxic conditions. Anaerobic metabolism is a logical mechanism to explain potential foraminiferal presence in suboxic layers. Complete or partial (with endo and/or ectobionts, Bernhard and Alve, 1996) denitrification co-occurring with nitrate storage has been proved (Risgaard-Petersen et al., 2006) for some foraminiferal taxa. However, despite intensive research efforts, no denitrification and no or a very low intracellular storage of nitrate has been observed in *A. tepida* (Geslin et al., 2014; Nomaki et al., 2014; Pina-Ochoa et al., 2010). This would suggest that suboxic deeper sediments cannot be considered as favorable environment for *A. tepida*. It implies that active colonization is probably not the explanation for the 3–8 cm depth density maximum.

4.3.2 Impact of macrofauna on *A. tepida* distribution

If it is clear that biomixing is a likely mechanism to explain the introduction of foraminifera in deeper sediment layers, by passive transport (Alve and Bernhard, 1995; Alve and Murray, 2001; Goldstein et al., 1995; Jorissen, 2003; Moodley et al., 1998; Saffert and Thomas, 1998). However, the spatial distribution resulting from this passive transport has never been well decribed, or modeled. According to the theory of biomixing, we suggest that the vertical distribution of *A. tepida* can be approached by a diffusion model (Fig. 10). If we accent the hypothesis of reproduction at the surface, the resulting profile should be an exponential decrease as drawn in Fig. 11 (dotted line). Possibly, *A. tepida* is able to survive in suboxic environment using an intermittent metabolism, using the oxygen that can be punctually available due to bioirrigation (Fenchel, 1996; Pischedda et al., 2012; Wang et al., 2001; Wenzhofer and Glud, 2004) in localized areas (Glud et al., 2009; Oguri et al., 2006). Figure 7c shows, between 1 and 3 cm depth, very low concentrations of dissolved iron at in some quadrants (e.g. B1–3), probably due to oxygen supply by bioirrigation. However, if the foraminifera found in suboxic/anoxic sediments depend on this intermittent oxygen supply, they have to reduce their metabolic activity in order to survive longer periods without oxygen supply. Their activity should progressively decrease once oxygen is depleted; Phipps (2012) suggested that they could eventually become immobilized before dyingin case of a prolonged absence of oxygen supply. We think that the reduced metabolic activity, eventually interrupted by incidental re-activation due to bioirrigation, is the most likely mechanism to explain the high abundance of living foraminifera in anoxic/suboxic sediments.

Figures 4a and 5b show no relation between visible burrows and living *A. tepida*. This result is in agreement with the idea that biomixing homogenizes the *A. tepida* density. It suggests also that the oxygenation obviously generated by new burrow formation is consumed too fast compared to the (reduced) *A. tepida* mobility in the surrounding environment. Thus, recent (visible) burrow walls do not provide a suitable niche for *A. tepida*, and can therefore not explain the observed centimeter heterogeneity of its density pattern. This result contrasts with earlier observations of higher foraminiferal densities (up to 300 times, rose bengal stained) in burrow walls. For example, data from burrows of *Amphicteis* sp. at 4800 m depth (Aller and Aller, 1986), of *Echiurus echiurus* at 42 m depth (Thomsen and Altenbach, 1993) and of *Pestarella tyrrhena* in intertidal sandflats (Koller et al., 2006) all present high foraminiferal densities. The observed differences could be due to the fact that burrows of various macrofaunal taxa may represent very different conditions and eventually to a difference in sampling scale, since (Koller et al., 2006; Thomsen and Altenbach, 1993) applied an irregular millimeter sampling around burrows. Finally, macrofaunal activity would explain transport to and survival in suboxic layers. However, this conceptual model cannot explain the lateral heterogeneity and the density minimum at 1–3 cm depth.

4.3.3 Sensitivity of *A. tepida* to geochemical gradients

To explain the 1–3 cm density minimum of *A. tepida*, we suggest an active upward migration of the specimens, back to the sediment surface, before they are completely immobilized by a lack of oxygen and a strongly lowered metabolism. Numerous studies have already reported that vertical migration of foraminifera allows them to move to more hospitable environments (Alve and Bernhard, 1995; Ernst et al., 2005; Geslin et al., 2004; Gross, 2000; Jorissen, 1988; Langezaal et al., 2003; Moodley et al., 1998; Van der Zwaan and Jorissen, 1991). In an experiment in which populations of *Haynesina germanica* were uniformly mixed in a 6 cm sediment column, Ernst et al. (2006) saw a clear migration back to the surface for the foraminifera living between 1 and 3 cm depth, and suggested that foraminifera living at greater depth were unable to do so. Similarly, Hess et al. (2013) showed that benthic foraminifera are able to migrate through suboxic sediment to reach oxic sediments over a maximal distance of a few centimeters. Active migration towards directly detected oxygen or organic matter over distances beyond 1 cm would be improbable, since this distance is much higher than the typical pseudopodial length (about 10 times the test diameter, see Travis and Rabalais, 1991). However, as described by the TEAP model, the presence of oxygen could be indirectly detected by other geochemical gradient (e.g. NO_3^-, Mn^{2+} or Fe^{2+}, DOM (dissolved organic matter), $p\mathrm{CO}_2$). This could explain the vertical migration of the foraminifera burrowed between 1 and 3 cm depth. Conversely, when gradients generated by the oxygen front are imperceptible for *A. tepida*, because they are living too deep in the sediment, or when such gradients are hidden by other sources of geochemical gradients (as organic-rich patches), this upward migration can no longer occur. This could explain why below 3 cm depth, *A. tepida* remains in the deeper sediment layer after being transported there accidentally. This incapacity to migrate back to the sediment surface generates the final profile presented in the Fig. 11.

However, the organization of the foraminiferal in 1 to 2 cm-wide horizontal patches suggests that *A. tepida* detects not only vertical geochemical gradients resulting from oxidant consumption by organic matter, but probably also lateral gradients around degrading biogenic particles. The characteristic length of patches of biogenic particles identified by dissolved iron (A/7–8, G–H/8–9 and F–G17 in Fig. 7c and d, see Sect. 4.2.2) and of the foraminiferal density maxima are in agreement. For the 8 first centimeters, the two identified biogenic particles (A/7–8, G–H/8–9) both correspond to a higher density of *A. tepida* (24 and 26 ind $\mathrm{cm^{-3}}$ in average for A/7–8 and G–H/8 respectively, Fig. 5b). It appears therefore that even in deeper suboxic layers, where foraminifera would have a lowered metabolism most of the time, they would have some capacity to move towards patches of labile organic matter. Nevertheless, a better identification of labile carbon patches, replicate sampling with the here developed strategy and experimental studies with artificial geochemical gradients are necessary to confirm our hypotheses about the behavior of *A. tepida* in suboxic environments.

5 Conclusion

We present a new, simple and robust sampling protocol, to obtain the 2-D distribution of benthic foraminifera. Our observations demonstrate a strong horizontal and vertical centime-scale patchiness of *A. tepida* in suboxic layers of “Les Brillantes” mudflat. This technique was coupled with a visual observation of burrow features and with an analysis of dissolved iron and DRP in 2-D allowing us to localize biogeochemical hotspots (due to bioirrigation or biogenic particle remineralisation). An overview of the mechanisms that likely control the distribution of *A tepida* suggests that it can be interpreted as the result of at least six interacting mechanisms (Fig. 11). (1) High foraminiferal densities at the surface are the result of reproduction in the oxygenated layer (Sect. 4.3.1), (2) passive downward transport by macrofaunal biomixing introduces living foraminfera in deeper sediment layers (Sect. 4.3.2), (3) in the 3 first centimeters foraminifera are capable to migrate back to the oxygenated, organic-rich surface layers once they detect redox gradients (Sect. 4.3.3), (4) in deeper sediment layers, they are no longer capable to find their way back to the superficial oxygenated layer probably because they can no longer detect geochemical gradients (Sect. 4.3.3), (5) after a prolonged presence in suboxic conditions, foraminifera lower their metabolism and become inactive, (6) foraminifera can become re-mobilizes during intermittent bioirrigation events, and can eventually migrate back to the surface or toward organic-rich microenvironments in their vicinity (Sect. 4.3.3). A systematical use of this practical, fast and cheap sampling method would better answer the questions evoked by the spatial heterogeneity reported here and in many previous studies.

The Supplement related to this article is available online at doi:10.5194/bgd-12-10311-2015-supplement.

Acknowledgements. This study is part of the RS2E-OSUNA project funded by the Région Pays de la Loire. Special thanks are due to Didier Jézéquel from IPGP that designed the “ jaw device”. Thanks to Clement Chauvin, Cyrille Guindir and Eve Chauveau for their support in the field.

References

Alldredge, A. L. and Cohen, Y.: Can microscale chemical patches persist in the sea? Microelectrode study of marine snow, fecal pellets, Science, 235, 689–691, doi:10.1126/science.235.4789.689, 1987.

Aller, J. Y. and Aller, R. C.: Evidence for localized enhancement of biological associated with tube and burrow structures in deep-sea sediments at the HEEBLE site, western North Atlantic, Deep-Sea Res., 33, 755–790, doi:10.1016/0198-0149(86)90088-9, 1986.

Aller, R. C.: The effects of macrobenthos on chemical properties of marine sediment and overlying water, in: Animal-Sediment Relations, edited by: McCall, P. L. and

Tevesz, M. J. S., Springer US, 53–102, available at: http://link.springer.com/chapter/10.1007/978-1-4757-1317-6_2 (last access: 22 August 2014), 1982.

Aller, R. C.: Conceptual models of early diagenetic processes: the muddy seafloor as an unsteady, batch reactor, J. Mar. Res., 62, 815–835, doi:10.1357/0022240042880837, 2004.

Aller, R. C.: 8.11 – sedimentary diagenesis, depositional environments, and benthic fluxes, in: Treatise on Geochemistry, 2nd edn., edited by: Turekian, H. D. H. K., Elsevier, Oxford, 293–334, available at: http://www.sciencedirect.com/science/article/pii/B9780080959757006112 (last access: 25 March 2015), 2014.

Alve, E. and Bernhard, J. M.: Vertical migratory response of benthic foraminifera to controlled oxygen concentrations in an experimental mesocosm, Oceanogr. Lit. Rev., 42, 137–151, doi:10.3354/meps116137, 1995.

Alve, E. and Murray, J. W.: Temporal variability in vertical distributions of live (stained) intertidal foraminifera, Southern England, J. Foramin. Res., 31, 12–24, doi:10.2113/0310012, 2001.

Anschutz, P., Zhong, S., Sundby, B., Mucci, A., and Gobeil, C.: Burial efficiency of phosphorus and the geochemistry of iron in continental margin sediments, Limnol. Oceanogr., 43, 53–64, 1998.

Anschutz, P., Dedieu, K., Desmazes, F., and Chaillou, G.: Speciation, oxidation state, and reactivity of particulate manganese in marine sediments, Chem. Geol., 218, 265–279, doi:10.1016/j.chemgeo.2005.01.008, 2005.

Arndt, S., Jørgensen, B. B., LaRowe, D. E., Middelburg, J. J., Pancost, R. D., and Regnier, P.: Quantifying the degradation of organic matter in marine sediments: a review and synthesis, Earth-Sci. Rev., 123, 53–86, doi:10.1016/j.earscirev.2013.02.008, 2013.

Barmawidjaja, D. M., Jorissen, F. J., Puskaric, S., and van der Zwaan, G. J.: Microhabitat selection by benthic Foraminifera in the northern Adriatic Sea, J. Foramin. Res., 22, 297–317, doi:10.2113/gsjfr.22.4.297, 1992.

Benyoucef, I.: Télédétection visible proche-infrarouge de la distribution spatio-temporelle du microphytobenthos estuarien, PhD thesis, Université de Nantes, 2014.

Benyoucef, I., Blandin, E., Lerouxel, A., Jesus, B., Rosa, P., Méléder, V., Launeau, P., and Barillé, L.: Microphytobenthos interannual variations in a north-European estuary (Loire estuary, France) detected by visible-infrared multispectral remote sensing, Estuar. Coast. Shelf S., 136, 43–52, doi:10.1016/j.ecss.2013.11.007, 2014.

Berg, P., Risgaard-Petersen, N., and Rysgaard, S.: Interpretation of measured concentration profiles in sediment pore water, Limnol. Oceanogr., 43, 1500–1510, doi:10.4319/lo.1998.43.7.1500, 1998.

Berkeley, A., Perry, C. T., Smithers, S. G., Horton, B. P., and Taylor, K. G.: A review of the ecological and taphonomic controls on foraminiferal assemblage development in intertidal environments, Earth-Sci. Rev., 83, 205–230, doi:10.1016/j.earscirev.2007.04.003, 2007.

Bernhard, J. M.: Benthic foraminiferal distribution and biomass related to pore-water oxygen content: central California continental slope and rise, Deep-Sea Res., 39, 585–605, doi:10.1016/0198-0149(92)90090-G, 1992.

Bernhard, J. M. and Alve, E.: Survival, ATP pool, and ultrastructural characterization of benthic foraminifera from Drammensfjord (Norway): response to anoxia, Mar. Micropaleontol., 28, 5–17, doi:10.1016/0377-8398(95)00036-4, 1996.

Bernhard, J. M. and Sen Gupta, B. K. S.: Foraminifera of oxygen-depleted environments, in: Modern Foraminifera, Springer Netherlands, 201–216, available at: http://link.springer.com/chapter/10.1007/0-306-48104-9_12 (last access: 27 November 2014), 2003.

Bernhard, J. M., Ostermann, D. R., Williams, D. S., and Blanks, J. K.: Comparison of two methods to identify live benthic foraminifera: a test between Rose Bengal and CellTracker Green with implications for stable isotope paleoreconstructions, Paleoceanography, 21, PA4210, doi:10.1029/2006PA001290, 2006.

Bernhard, J. M., Edgcomb, V. P., Casciotti, K. L., McIlvin, M. R., and Beaudoin, D. J.: Denitrification likely catalyzed by endobionts in an allogromiid foraminifer, ISME J., 6, 951–960, doi:10.1038/ismej.2011.171, 2012.

Bivand, R., Pebesma, E., and Gomez-Rubio, V.: Applied Spatial Data Analysis with R, Springer New York, New York, NY, available at: http://link.springer.com/10.1007/978-0-387-78171-6 (last access: 16 August 2014), 2008.

Blanchard, G.: Overlapping microscale dispersion patterns of meiofauna and microphytobenthos, Mar. Ecol.-Prog. Ser., 68, 101–111, doi:10.3354/meps068101, 1990.

Borcard, D., Gillet, F., and Legendre, P.: Numerical Ecology with R, Springer New York, New York, NY, available at: http://link.springer.com/10.1007/978-1-4419-7976-6 (last access: 16 August 2014), 2011.

Bouchet, V. M. P., Sauriau, P.-G., Debenay, J.-P., Mermillod-Blondin, F., Schmidt, S., Amiard, J.-C., and Dupas, B.: Influence of the mode of macrofauna-mediated bioturbation on the vertical distribution of living benthic foraminifera: first insight from axial tomodensitometry, J. Exp. Mar. Biol. Ecol., 371, 20–33, doi:10.1016/j.jembe.2008.12.012, 2009.

Boudreau, B. P.: A method-of-lines code for carbon and nutrient diagenesis in aquatic sediments, Comput. Geosci., 22, 479–496, 1996.

Buzas, M. A.: On the spatial distribution of foraminifera, Contrib. Cushman Found. Foramin. Res., 19, 1–11, 1968.

Buzas, M. A.: Spatial homogeneity: statistical analyses of unispecies and multispecies populations of foraminifera, Ecology, 51, 874, doi:10.2307/1933980, 1970.

Buzas, M. A., Hayek, L.-A. C., Reed, S. A., and Jett, J. A.: Foraminiferal densities over five years in the Indian River Lagoon, Florida: a model of pulsating patches, J. Foramin. Res., 32, 68–92, doi:10.2113/0320068, 2002.

Cesbron, F., Metzger, E., Launeau, P., Deflandre, B., Delgard, M.-L., Thibault de Chanvalon, A., Geslin, E., Anschutz, P., and Jézéquel, D.: Simultaneous 2D imaging of dissolved iron and reactive phosphorus in sediment porewaters by thin-film and hyperspectral methods, Environ. Sci. Technol., 48, 2816–2826, doi:10.1021/es404724r, 2014.

Chandler, G. T.: Foraminifera may structure meiobenthic communities, Oecologia, 81, 354–360, doi:10.1007/BF00377083, 1989.

Davison, W. and Zhang, H.: In situspeciation measurements of trace components in natural waters using thin-film gels, Nature, 367, 546–548, doi:10.1038/367546a0, 1994.

De Nooijer, L. J.: Shallow-water benthic foraminifera as proxy for natural versus human-induced environmental change, Utrecht University, available at: http://epic.awi.de/20976/1/de2007h.pdf (last access: 25 September 2014), 2007.

Debenay, J.-P. and Guillou, J.-J.: Ecological transitions indicated by foraminiferal assemblages in paralic environments, Estuaries, 25, 1107–1120, doi:10.1007/BF02692208, 2002.

Debenay, J.-P., Bicchi, E., Goubert, E., and Armynot du Châtelet, E.: Spatio-temporal distribution of benthic foraminifera in relation to estuarine dynamics (Vie estuary, Vendée, W France), Estuar. Coast. Shelf S., 67, 181–197, doi:10.1016/j.ecss.2005.11.014, 2006.

Duport, E., Stora, G., Tremblay, P., and Gilbert, F.: Effects of population density on the sediment mixing induced by the gallery-diffusor *Hediste (Nereis) diversicolor* O.F. Müller, 1776, J. Exp. Mar. Biol. Ecol., 336, 33–41, doi:10.1016/j.jembe.2006.04.005, 2006.

Eckman, J. E. and Thistle, D.: Small-scale spatial pattern in meiobenthos in the San Diego Trough, Deep-Sea Res., 35, 1565–1578, doi:10.1016/0198-0149(88)90103-3, 1988.

Ernst, S., Bours, R., Duijnstee, I., and van der Zwaan, B.: Experimental effects of an organic matter pulse and oxygen depletion on a benthic foraminiferal shelf community, J. Foramin. Res., 35, 177–197, 2005.

Ernst, S. R., Morvan, J., Geslin, E., Le Bihan, A., and Jorissen, F. J.: Benthic foraminiferal response to experimentally induced Erika oil pollution, Mar. Micropaleontol., 61, 76–93, doi:10.1016/j.marmicro.2006.05.005, 2006.

Fenchel, T.: Worm burrows and oxic microniches in marine sediments. 1. Spatial and temporal scales, Mar. Biol., 127, 289–295, doi:10.1007/BF00942114, 1996.

Findlay, S. E. G.: Small-scale spatial distribution ofmeiofauna on a mud- and sandflat, Estuar. Coast. Shelf S., 12, 471–484, doi:10.1016/S0302-3524(81)80006-0, 1981.

Le Floch, J.-F.: Propagation de la marée dynamique dans l'estuaire de la Seine et en Seine maritime, Thèse d'Etat, Université de Paris, 1961

Fontanier, C., Jorissen, F. J., Licari, L., Alexandre, A., Anschutz, P., and Carbonel, P.: Live benthic foraminiferal faunas from the Bay of Biscay: faunal density, composition, and microhabitats, Deep-Sea Res., 49, 751–785, doi:10.1016/S0967-0637(01)00078-4, 2002.

Fortin, M.-J. and Dale, M. R. T.: Spatial Analysis a Guide for Ecologists, Cambridge University Press, Cambridge, NY, availbale at: http://public.eblib.com/EBLPublic/PublicView.do?ptiID=228304 (last access: 16 August 2014), 2005.

François, F., Gerino, M., Stora, G., Durbec, J., and Poggiale, J.: Functional approach to sediment reworking by gallery-forming macrobenthic organisms: modeling and application with the polychaete Nereis diversicolor, Mar. Ecol.-Prog. Ser., 229, 127–136, doi:10.3354/meps229127, 2002.

Froelich, P. N., Klinkhammer, G. P., Bender, M. L., Luedtke, N. A., Heath, G. R., Cullen, D., Dauphin, P., Hammond, D., Hartman, B., and Maynard, V.: Early oxidation of organic matter in pelagic sediments of the eastern equatorial Atlantic: suboxic diagenesis, Geochim. Cosmochim. Ac., 43, 1075–1090, doi:10.1016/0016-7037(79)90095-4, 1979.

Geslin, E., Heinz, P., Jorissen, F., and Hemleben, C.: Migratory responses of deep-sea benthic foraminifera to variable oxygen conditions: laboratory investigations, Mar. Micropaleontol., 53, 227–243, doi:10.1016/j.marmicro.2004.05.010, 2004.

Geslin, E., Barras, C., Langlet, D., Nardelli, M. P., Kim, J.-H., Bonnin, J., Metzger, E., and Jorissen, F. J.: Survival, reproduction and calcification of three benthic foraminiferal species in response to experimentally induced hypoxia, in: Approaches to Study Living Foraminifera, edited by: Kitazato, H. and Bernhard, J. M., Springer Japan, 163–193, available at: http://link.springer.com/chapter/10.1007/978-4-431-54388-6_10, last access: 20 August 2014.

Gillet, P., Mouloud, M., Mouneyrac, C., Simo, P., and Gilbert, F.: Preliminary data on the bioturbation activity of *hediste diversicolor* (polychaeta, nereididae) from the Loire Estuary, France, Open Mar. Biol. J., 6, 53–56, 2012.

Glud, R. N., Stahl, H., Berg, P., Wenzhofer, F., Oguri, K., and Kitazato, H.: In situ microscale variation in distribution and consumption of O_2: a case study from a deep ocean margin sediment (Sagami Bay, Japan), Limnol. Oceanogr., 54, 1–12, doi:10.4319/lo.2009.54.1.0001, 2009.

Goldstein, S. T., Watkins, G. T., and Kuhn, R. M.: Microhabitats of salt marsh foraminifera: St. Catherines Island, Georgia, USA, Mar. Micropaleontol., 26, 17–29, doi:10.1016/0377-8398(95)00006-2, 1995.

Gross, O.: Influence of temperature, oxygen and food availability on the migrational activity of bathyal benthic foraminifera: evidence by microcosm experiments, in: Life at Interfaces and Under Extreme Conditions, edited by Liebezeit, G., Dittmann, S., and Kröncke, I., Springer Netherlands, 123–137, available at: http://link.springer.com/chapter/10.1007/978-94-011-4148-2_12 (last access: 3 October 2014), 2000.

Hebert, A. B., Morse, J. W., and Eldridge, P. M.: Small-scale heterogeneity in the geochemistry of seagrass vegetated and non-vegetated estuarine sediments: causes and consequences, Aquat. Geochem., 13, 19–39, doi:10.1007/s10498-006-9007-3, 2007.

Heinz, P. and Geslin, E.: Ecological and biological response of benthic foraminifera under oxygen-depleted conditions: evidence from laboratory approaches, in: Anoxia, edited by: Altenbach, A. V., Bernhard, J. M., and Seckbach, J., Springer Netherlands, 287–303, available at: http://link.springer.com/chapter/10.1007/978-94-007-1896-8_15 (last access: 7 January 2015), 2012.

Hess, S., Alve, E., Trannum, H. C., and Norling, K.: Benthic foraminiferal responses to water-based drill cuttings and natural sediment burial: results from a mesocosm experiment, Mar. Micropaleontol., 101, 1–9, doi:10.1016/j.marmicro.2013.03.004, 2013.

Hofmann, A. F., Soetaert, K., Middelburg, J. J., and Meysman, F. J. R.: AquaEnv?: an aquatic acid–base modelling environment in R, Aquat. Geochem., 16, 507–546, doi:10.1007/s10498-009-9084-1, 2010.

Hohenegger, J., Piller, W., and Baal, C.: Reasons for spatial microdistributions of foraminifers in an intertidal pool (northern Adriatic Sea), Mar. Ecol.-Evol. Persp., 10, 43–78, 1989.

Hohenegger, J., Piller, W. E., and Baal, C.: Horizontal and vertical spatial microdistribution of foraminifers in the shallow subtidal Gulf of Trieste, northern Adriatic Sea, J. Foramin. Res., 23, 79–101, doi:10.2113/gsjfr.23.2.79, 1993.

Hyacinthe, C. and Van Cappellen, P.: An authigenic iron phosphate phase in estuarine sediments: composition, formation and chemical reactivity, Mar. Chem., 91, 227–251, doi:10.1016/j.marchem.2004.04.006, 2004.

Hyacinthe, C., Anschutz, P., Carbonel, P., Jouanneau, J.-M., and Jorissen, F. J.: Early diagenetic processes in the muddy sediments of the Bay of Biscay, Mar. Geol., 177, 111–128, doi:10.1016/S0025-3227(01)00127-X, 2001.

Hyacinthe, C., Bonneville, S., and Van Cappellen, P.: Reactive iron(III) in sediments: chemical versus Microbial extractions, Geochim. Cosmochim. Ac., 70, 4166–4180, doi:10.1016/j.gca.2006.05.018, 2006.

Jorissen, F. J.: Benthic foraminifera from the Adriatic Sea: principles of phenotypic variation, Utrecht Micropaleontological Bulletins, 37, 174 pp., 1988.

Jorissen, F. J.: Benthic foraminiferal microhabitats below the sediment–water interface, in: Modern Foraminifera, Springer Netherlands,161–179, available at: http://link.springer.com/chapter/10.1007/0-306-48104-9_10 (last access: 20 August 2014), 2003.

Jorissen, F. J., Barmawidjaja, D. M., Puskaric, S., and van der Zwaan, G. J.: Vertical distribution of benthic foraminifera in the northern Adriatic Sea: the relation with the organic flux, Mar. Micropaleontol., 19, 131–146, doi:10.1016/0377-8398(92)90025-F, 1992.

Jorissen, F. J., de Stigter, H. C., and Widmark, J. G. V.: A conceptual model explaining benthic foraminiferal microhabitats, Mar. Micropaleontol., 26, 3–15, doi:10.1016/0377-8398(95)00047-X, 1995.

Jorissen, F. J., Wittling, I., Peypouquet, J. P., Rabouille, C., and Relexans, J. C.: Live benthic foraminiferal faunas off Cape Blanc, NW-Africa: community structure and microhabitats, Deep-Sea Res., 45, 2157–2188, doi:10.1016/S0967-0637(98)00056-9, 1998.

Koller, H., Dworschak, P. C., and Abed-Navandi, D.: Burrows of *Pestarella tyrrhena* (Decapoda: Thalassinidea): hot spots for Nematoda, Foraminifera and bacterial densities, J. Mar. Biol. Assoc. UK, 86, 1113–1122, 2006.

Kostka, J. E. and Luther III, G. W.: Partitioning and speciation of solid phase iron in saltmarsh sediments, Geochim. Cosmochim. Ac., 58, 1701–1710, doi:10.1016/0016-7037(94)90531-2, 1994.

Kostka, J. E. and Luther III, G. W.: Seasonal cycling of Fe in saltmarsh sediments, Biogeochemistry, 29, 159–181, 1995.

Kristensen, E., PenhaLopes, G., Delefosse, M., Valdemarsen, T., Quintana, C. O., and Banta, G. T.: REVIEW What is bioturbation? The need for a precise definition for fauna in aquatic sciences, Mar. Ecol.-Prog. Ser., 446, 285–302, doi:10.3354/meps09506, 2012.

Krom, M. D., Davison, P., Zhang, H., and Davison, W.: High-resolution pore-water sampling with a gel sampler, Limnol. Oceanogr., 39, 1967–1972, 1994.

Langezaal, A. M., Ernst, S. R., Haese, R. R., van Bergen, P. F., and van der Zwaan, G. J.: Disturbance of intertidal sediments: the response of bacteria and foraminifera, Estuar. Coast. Shelf S., 58, 249–264, doi:10.1016/S0272-7714(03)00078-7, 2003.

Langezaal, A. M., Jorissen, F. J., Braun, B., Chaillou, G., Fontanier, C., Anschutz, P., and van der Zwaan, G. J.: The influence of seasonal processes on geochemical profiles and foraminiferal assemblages on the outer shelf of the Bay of Biscay, Cont. Shelf Res., 26, 1730–1755, doi:10.1016/j.csr.2006.05.005, 2006.

Langlet, D., Geslin, E., Baal, C., Metzger, E., Lejzerowicz, F., Riedel, B., Zuschin, M., Pawlowski, J., Stachowitsch, M., and Jorissen, F. J.: Foraminiferal survival after long-term in situ experimentally induced anoxia, Biogeosciences, 10, 7463–7480, doi:10.5194/bg-10-7463-2013, 2013.

Legendre, P. and Fortin, M.-J.: Spatial pattern and ecological analysis, Vegetation, 80, 107–138, 1989.

Legendre, P. and Fortin, M.-J.: Comparison of the Mantel test and alternative approaches for detecting complex multivariate relationships in the spatial analysis of genetic data, Mol. Ecol. Resour., 10, 831–844, doi:10.1111/j.1755-0998.2010.02866.x, 2010.

Leutenegger, S. and Hansen, H. J.: Ultrastructural and radiotracer studies of pore function in foraminifera, Mar. Biol., 54, 11–16, doi:10.1007/BF00387046, 1979.

Lewandowski, J. and Hupfer, M.: Effect of macrozoobenthos on two-dimensional small-scale heterogeneity of pore water phosphorus concentrations in lake sediments: a laboratory study, Limnol. Oceanogr., 50, 1106–1118, 2005.

Lewandowski, J., Rüter, K., and Hupfer, M.: Two-dimensional small-scale variability of pore water phosphate in freshwater lakes: results from a novel dialysis sampler, Environ. Sci. Technol., 36, 2039–2047, doi:10.1021/es0102538, 2002.

Loubere, P., Jacobsen, B., Klitgaard Kristensen, D., Husum, K., Jernas, P., and Richaud, M.: The structure of benthic environments and the paleochemical record of foraminifera, Deep-Sea Res., 58, 535–545, doi:10.1016/j.dsr.2011.02.011, 2011.

Lynts, G. W.: Relationship of sediment-size distribution to ecologic factors in Buttonwood Sound, Florida Bay, J. Sediment. Res., 36, 66–74, 1966.

Martiny, J. B. H., Bohannan, B. J. M., Brown, J. H., Colwell, R. K., Fuhrman, J. A., Green, J. L., Horner-Devine, M. C., Kane, M., Krumins, J. A., Kuske, C. R., Morin, P. J., Naeem, S., Øvreås, L., Reysenbach, A.-L., Smith, V. H., and Staley, J. T.: Microbial biogeography: putting microorganisms on the map, Nat. Rev. Microbiol., 4, 102–112, doi:10.1038/nrmicro1341, 2006.

Meyers, M. B., Fossing, H. and Powel, E. N.: Microdistribution of interstitial meiofauna, oxygen and sulfide gradients, and the tubes of macro-infauna, Mar. Ecol.-Prog. Ser., 35, 223–241, doi:10.3354/meps035223, 1987.

Metzger, E., Simonucci, C., Viollier, E., Sarazin, G., Prévot, F., and Jézéquel, D.: Benthic response to shellfish farming in Thau lagoon: pore water signature, Estuar. Coast. Shelf S., 72, 406–419, doi:10.1016/j.ecss.2006.11.011, 2007.

Metzger, E., Langlet, D., Viollier, E., Koron, N., Riedel, B., Stachowitsch, M., Faganeli, J., Tharaud, M., Geslin, E., and Jorissen, F.: Artificially induced migration of redox layers in a coastal sediment from the Northern Adriatic, Biogeosciences, 11, 2211–2224, doi:10.5194/bg-11-2211-2014, 2014.

Meysman, F. J. R., Boudreau, B. P., and Middelburg, J. J.: Relations between local, nonlocal, discrete and continuous models of bioturbation, J. Mar. Res., 61, 391–410, doi:10.1357/002224003322201241, 2003.

Meysman, F. J. R., Middelburg, J. J., and Heip, C. H. R.: Bioturbation: a fresh look at Darwin's last idea, Trends Ecol. Evol., 21, 688–695, doi:10.1016/j.tree.2006.08.002, 2006.

Meysman, F. J. R., Malyuga, V. S., Boudreau, B. P., and Middelburg, J. J.: A generalized stochastic approach to particle dispersal in soils and sediments, Geochim. Cosmochim. Ac., 72, 3460–3478, doi:10.1016/j.gca.2008.04.023, 2008.

Meysman, F. J. R., Boudreau, B. P., and Middelburg, J. J.: When and why does bioturbation lead to diffusive mixing?, J. Mar. Res., 68, 881–920, 2010a.

Meysman, F. J. R., Galaktionov, O. S., Glud, R. N., and Middelburg, J. J.: Oxygen penetration around burrows and roots in aquatic sediments, J. Mar. Res., 68, 309–336, doi:10.1357/002224010793721406, 2010b.

Millero, F. J.: The thermodynamics of the carbonate system in seawater, Geochim. Cosmochim. Ac., 43, 1651–1661, doi:10.1016/0016-7037(79)90184-4, 1979.

Millero, F. J.: Thermodynamics of the carbon dioxide system in the oceans, Geochim. Cosmochim. Ac., 59, 661–677, doi:10.1016/0016-7037(94)00354-O, 1995.

Moodley, L.: Southern North Sea seafloor and subsurface distribution of living benthic foraminifera, Neth. J. Sea Res., 27, 57–71, doi:10.1016/0077-7579(90)90034-E, 1990.

Moodley, L. and Hess, C.: Tolerance of infaunal benthic foraminifera for low and high oxygen concentrations, Biol. Bull., 183, 94–98, 1992.

Moodley, L., van der Zwaan, G. J., Rutten, G. M. W., Boom, R. C. E., and Kempers, A. J.: Subsurface activity of benthic foraminifera in relation to porewater oxygen content: laboratory experiments, Mar. Micropaleontol., 34, 91–106, doi:10.1016/S0377-8398(97)00044-3, 1998.

Morse, J. W., DiMarco, S. F., Hebert, A. B., and Sell, K. S.: A scaling approach to spatial variability in early diagenetic processes, in: The Interactions Between Sediments and Water, Springer, 25–29, available at: http://link.springer.com/chapter/10.1007/978-94-017-3366-3_5 (last access: 30 June 2014), 2003.

Morvan, J., Debenay, J.-P., Jorissen, F., Redois, F., Bénéteau, E., Delplancke, M., and Amato, A.-S.: Patchiness and life cycle of intertidal foraminifera: implication for environmental and paleoenvironmental interpretation, Mar. Micropaleontol., 61, 131–154, doi:10.1016/j.marmicro.2006.05.009, 2006.

Mucci, A.: The solubility of calcite and aragonite in seawater at various salinities, temperatures, and one atmosphere total pressure, Am. J. Sci., 283, 780–799, doi:10.2475/ajs.283.7.780, 1983.

Mucci, A., Sundby, B., Gehlen, M., Arakaki, T., Zhong, S., and Silverberg, N.: The fate of carbon in continental shelf sediments of eastern Canada: a case study, Deep-Sea Res. Pt. II, 47, 733–760, doi:10.1016/S0967-0645(99)00124-1, 2000.

Nardelli, M. P., Barras, C., Metzger, E., Mouret, A., Filipsson, H. L., Jorissen, F., and Geslin, E.: Experimental evidence for foraminiferal calcification under anoxia, Biogeosciences, 11, 4029–4038, doi:10.5194/bg-11-4029-2014, 2014.

Nomaki, H., Chikaraishi, Y., Tsuchiya, M., Toyofuku, T., Ohkouchi, N., Uematsu, K., Tame, A., and Kitazato, H.: Nitrate uptake by foraminifera and use in conjunction with endobionts under anoxic conditions, Limnol. Oceanogr., 59, 1879–1888, doi:10.4319/lo.2014.59.6.1879, 2014.

Oguri, K., Kitazato, H., and Glud, R. N.: Platinum octaetylporphyrin based planar optodes combined with an UV-LED excitation light source: an ideal tool for high-resolution O_2 imaging in

O_2 depleted environments, Mar. Chem., 100, 95–107, doi:10.1016/j.marchem.2005.11.005, 2006.

Olsson, I. and Eriksson, B.: Horizontal distribution of meiofauna within a small area, with special reference to Foraminifera, Zoon, 2, 67–84, 1974.

Phipps, M. D.: benthic foraminifera of the Portuguese margin: impact of organic supplies on the density, biodiversity and composition of the faunas, Université d'Angers, available at: https://tel.archives-ouvertes.fr/tel-00993121/ (last access: 28 April 2015), 2012.

Pina-Ochoa, E., Hogslund, S., Geslin, E., Cedhagen, T., Revsbech, N. P., Nielsen, L. P., Schweizer, M., Jorissen, F., Rysgaard, S., and Risgaard-Petersen, N.: Widespread occurrence of nitrate storage and denitrification among Foraminifera and Gromiida, P. Natl. Acad. Sci. USA, 107, 1148–1153, doi:10.1073/pnas.0908440107, 2010.

Pischedda, L., Cuny, P., Esteves, J. L., Poggiale, J.-C., and Gilbert, F.: Spatial oxygen heterogeneity in a Hediste diversicolor irrigated burrow, Hydrobiologia, 680, 109–124, doi:10.1007/s10750-011-0907-x, 2012.

Pucci, F., Geslin, E., Barras, C., Morigi, C., Sabbatini, A., Negri, A., and Jorissen, F. J.: Survival of benthic foraminifera under hypoxic conditions: results of an experimental study using the CellTracker Green method, Mar. Pollut. Bull., 59, 336–351, doi:10.1016/j.marpolbul.2009.08.015, 2009.

Revsbech, N. P., SøRensen, J., Blackburn, T. H., and Lomholt, J. P.: Distribution of oxygen in marine sediments measured with microelectrodes, Limnol. Oceanogr., 25, 403–411, doi:10.4319/lo.1980.25.3.0403, 1980.

Richter, G.: Beobachtungen zur Ökologie einiger Foraminiferen des Jade Gebietes, Nat. Volk, 91, 163–170, 1961.

Risgaard-Petersen, N., Langezaal, A. M., Ingvardsen, S., Schmid, M. C., Jetten, M. S. M., Op den Camp, H. J. M., Derksen, J. W. M., Piña-Ochoa, E., Eriksson, S. P., Nielsen, L. P., Revsbech, N. P., Cedhagen, T., and van der Zwaan, G. J.: Evidence for complete denitrification in a benthic foraminifer, Nature, 443, 93–96, doi:10.1038/nature05070, 2006.

Robertson, D., Welsh, D. T., and Teasdale, P. R.: Investigating biogenic heterogeneity in coastal sediments with two-dimensional measurements of iron(II) and sulfide, Environ. Chem., 6, 60–69, 2009.

Saffert, H. and Thomas, E.: Living foraminifera and total populations in salt marsh peat cores: Kelsey Marsh (Clinton, CT) and the Great Marshes (Barnstable, MA), Mar. Micropaleontol., 33, 175–202, doi:10.1016/S0377-8398(97)00035-2, 1998.

Santner, J., Larsen, M., Kreuzeder, A., and Glud, R. N.: Two decades of chemical imaging of solutes in sediments and soils – a review, Anal. Chim. Acta, 878, 9–42, doi:10.1016/j.aca.2015.02.006, 2015.

Schiffers, K., Teal, L. R., Travis, J. M. J., and Solan, M.: An open source simulation model for soil and sediment bioturbation, PLoS ONE, 6, e28028, doi:10.1371/journal.pone.0028028, 2011.

De Stigter, H. C., van der Zwaan, G. J., and Langone, L.: Differential rates of benthic foraminiferal test production in surface and subsurface sediment habitats in the southern Adriatic Sea, Palaeogeogr. Palaeocl., 149, 67–88, doi:10.1016/S0031-0182(98)00193-X, 1999.

Stockdale, A., Davison, W., and Zhang, H.: Micro-scale biogeochemical heterogeneity in sediments: a review of available technology and observed evidence, Earth-Sci. Rev., 92, 81–97, doi:10.1016/j.earscirev.2008.11.003, 2009.

Stockdale, A., Davison, W., and Zhang, H.: Formation of iron sulfide at faecal pellets and other microniches within suboxic surface sediment, Geochim. Cosmochim. Ac., 74, 2665–2676, doi:10.1016/j.gca.2010.02.005, 2010.

Thomsen, L. and Altenbach, A. V.: Vertical and areal distribution of foraminiferal abundance and biomass in microhabitats around inhabited tubes of marine echiurids, Mar. Micropaleontol., 20, 303–309, doi:10.1016/0377-8398(93)90039-Z, 1993.

Travis, J. L. and Rabalais, N. N.: The motility of foraminifera, in: Biology of the Foraminifera, edited by: Lee, J. J. and Anderson, O. R., Academic Press, London, 91–155, 1991.

Wang, F., Tessier, A., and Hare, L.: Oxygen measurements in the burrows of freshwater insects, Freshwater Biol., 46, 317–327, 2001.

Wenzhofer, F. and Glud, R. N.: Small-scale spatial and temporal variability in coastal benthic O_2 dynamics: effects of fauna activity, Limnol. Oceanogr., 49, 1471–1481, 2004.

Wheatcroft, R. A., Jumars, P. A., Smith, C. R., and Nowell, A. R. M.: A mechanistic view of the particulate biodiffusion coefficient: step lengths, rest periods and transport directions, J. Mar. Res., 48, 177–207, 1990.

Wu, J., Jelinski, D. E., Luck, M., and Tueller, P. T.: Multiscale analysis of landscape heterogeneity: scale variance and pattern metrics, Geogr. Inf. Sci., 6, 6–19, doi:10.1080/10824000009480529, 2000.

Zhu, Q. and Aller, R. C.: Two-dimensional dissolved ferrous iron distributions in marine sediments as revealed by a novel planar optical sensor, Mar. Chem., 136–137, 14–23, doi:10.1016/j.marchem.2012.04.002, 2012.

Zhu, Q., Aller, R. C., and Fan, Y.: Two-dimensional pH distributions and dynamics in bioturbated marine sediments, Geochim. Cosmochim. Ac., 70, 4933–4949, doi:10.1016/j.gca.2006.07.033, 2006.

Zorn, M. E., Lalonde, S. V., Gingras, M. K., Pemberton, S. G., and Konhauser, K. O.: Microscale oxygen distribution in various invertebrate burrow walls, Geobiology, 4, 137–145, doi:10.1111/j.1472-4669.2006.00074.x, 2006.

Van der Zwaan, G. J. and Jorissen, F. J.: Biofacial patterns in river-induced shelf anoxia, Geol. Soc. Lond. Spec. Publ., 58, 65–82, doi:10.1144/GSL.SP.1991.058.01.05, 1991.

Van der Zwaan, G. J., Duijnstee, I. A. P., den Dulk, M., Ernst, S. R., Jannink, N. T., and Kouwenhoven, T. J.: Benthic foraminifers: proxies or problems?: a review of paleocological concepts, Earth-Sci. Rev., 46, 213–236, doi:10.1016/S0012-8252(99)00011-2, 1999.

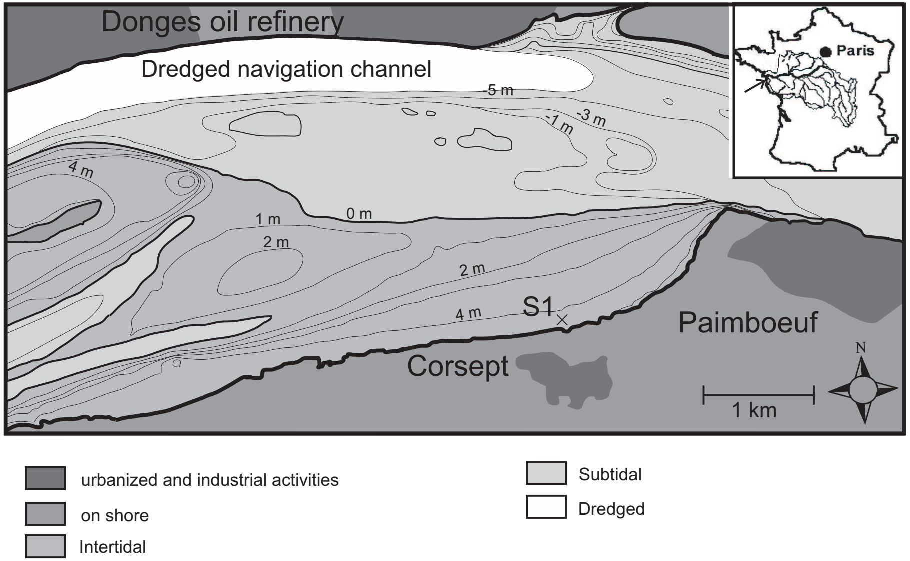

Figure 1. Location of sampling station S1 in the mudflat of “Les Brillantes” in the Loire Estuary (France).

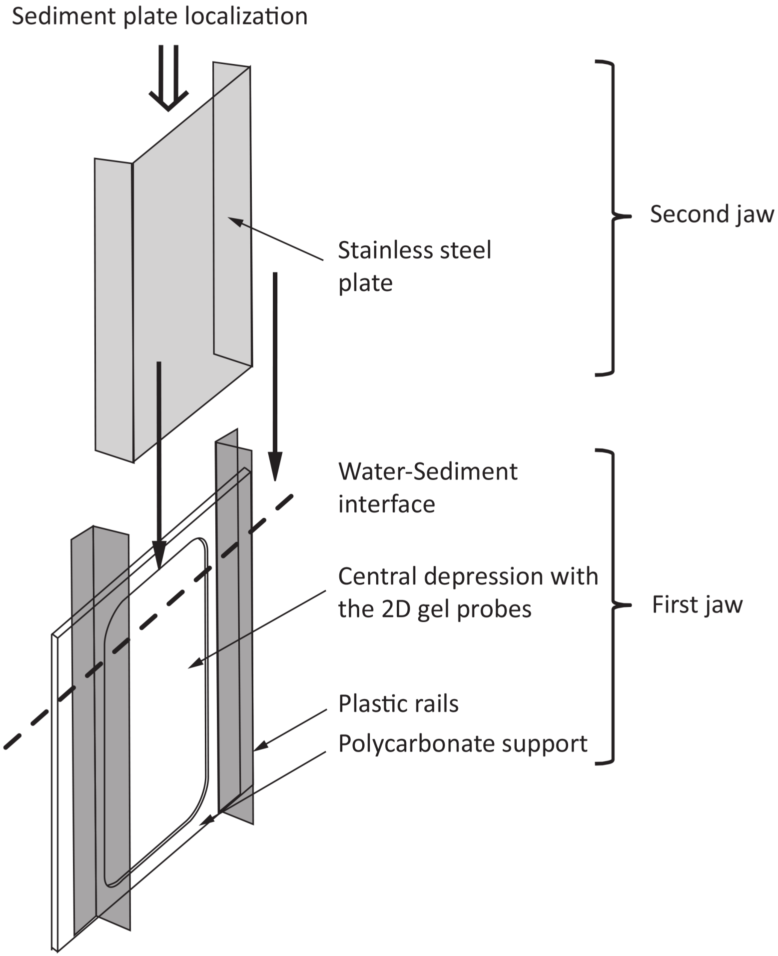

Figure 2. Schematic view of the “jaw device” for simultaneous sampling sediment and porewater.

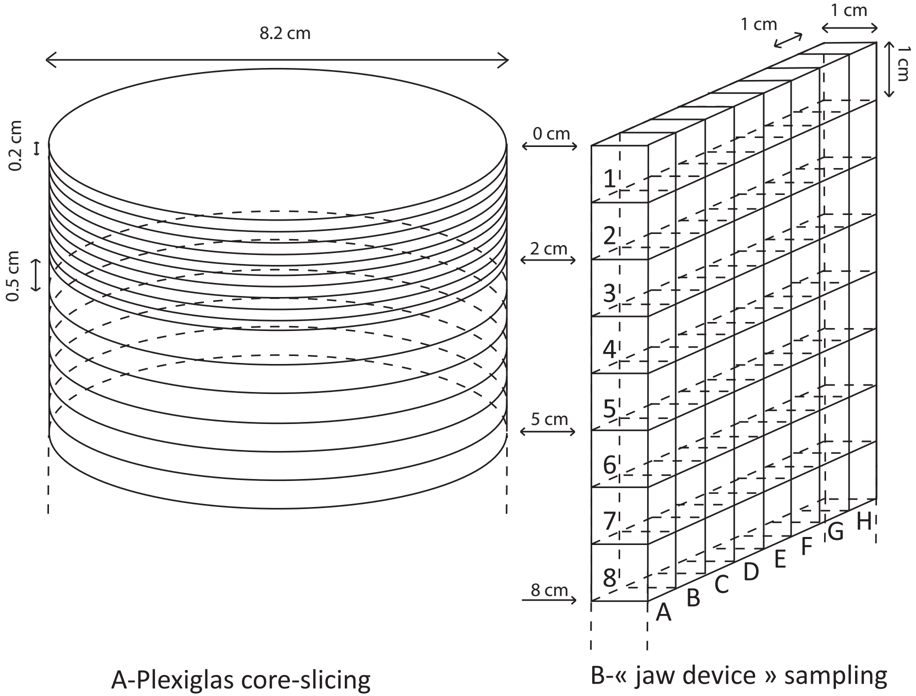

Figure 3. Sediment sampling methodologies for living foraminiferal analyses. **(a)** Usual 1-D hand coring and layer slicing. **(b)** Sediment plate sampling with the second jaw of “jaw device” (Fig. 2) and representation of the sediment cubic slicing.

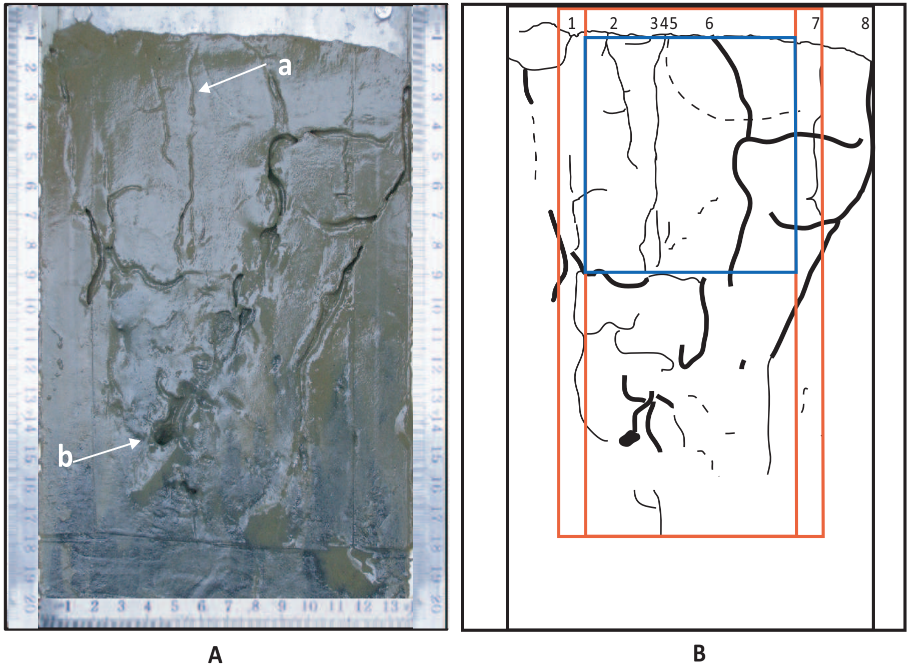

Figure 4. (a) Picture of the sediment plate before the slicing in cubes for foraminiferal analysis. Sediment water interface is at the top. Arrows "a" and "b" represent burrow in the cutting plan and in a perpendicular plan respectively. **(b)** Sediment visual interpretation with boundaries of dissolved analysis (exterior red line for gel boundaries and interior red line for exploitable data), boundary of foraminifera counting (blue line), apparent burrows (black/grey/dashed line following their thickness and numbering of those connected to the surface).

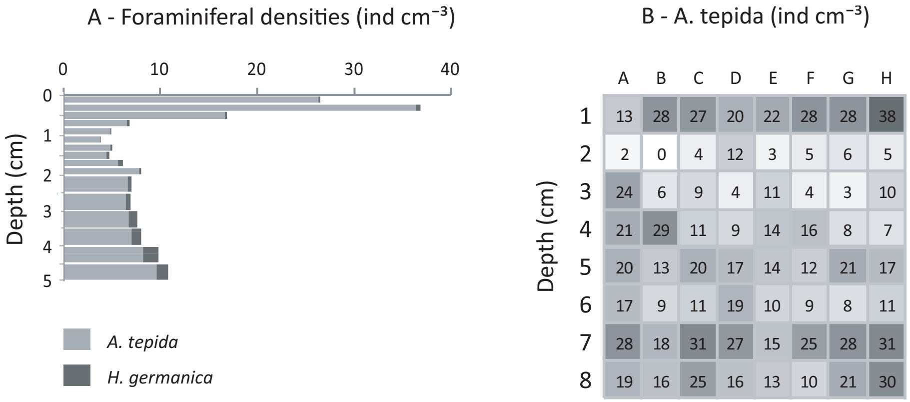

	A	B	C	D	E	F	G	H
1	13	28	27	20	22	28	28	38
2	2	0	4	12	3	5	6	5
3	24	6	9	4	11	4	3	10
4	21	29	11	9	14	16	8	7
5	20	13	20	17	14	12	21	17
6	17	9	11	19	10	9	8	11
7	28	18	31	27	15	25	28	31
8	19	16	25	16	13	10	21	30

Figure 5. (a) Vertical profile of living foraminiferal densities from the sliced core (ø = 8.2 cm). **(b)** 2-D distribution of *A. tepida* densities from the sediment plate with visual interpretation (Fig. 4b).

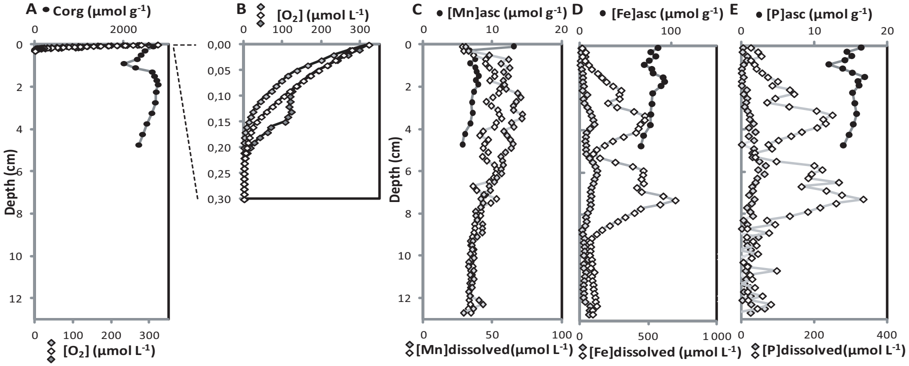

Figure 6. 1-D geochemical features. **(a)** Vertical profile of total solid organic carbon (filled circles, incertitude smaller than symbol size) and profiles of dissolved oxygen (open diamonds). **(b)** Typical profiles of dissolved oxygen, dark grey diamond profile is considered as bioturbated. **(c–e)** Vertical profiles of manganese **(c)**, iron **(d)** and phosphorus **(e)** in dissolved (white and gray diamonds for DET replicates) and reactive solid phase (ascorbate-leached) from the core (black circles).

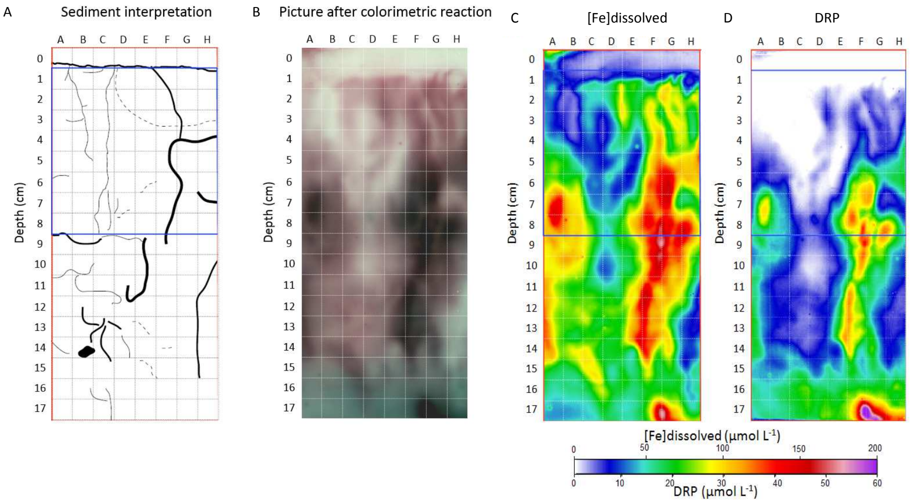

Figure 7. (a) Visual interpretation of the sediment picture as presented in the Fig. 4b, with italic numbers identifying burrows connected to the surface according to the Fig. 4b. **(b)** Picture of the analyzed gel after colorimetric reactions: dissolved iron shows in dark pink and dissolved phosphorus in turquoise. (**c** and **d**) Two dimension concentrations after numerical analysis of dissolved iron and dissolved reactive phosphorus (DRP) colored reactions. Blue lines represent boundary of foraminifera analysis.

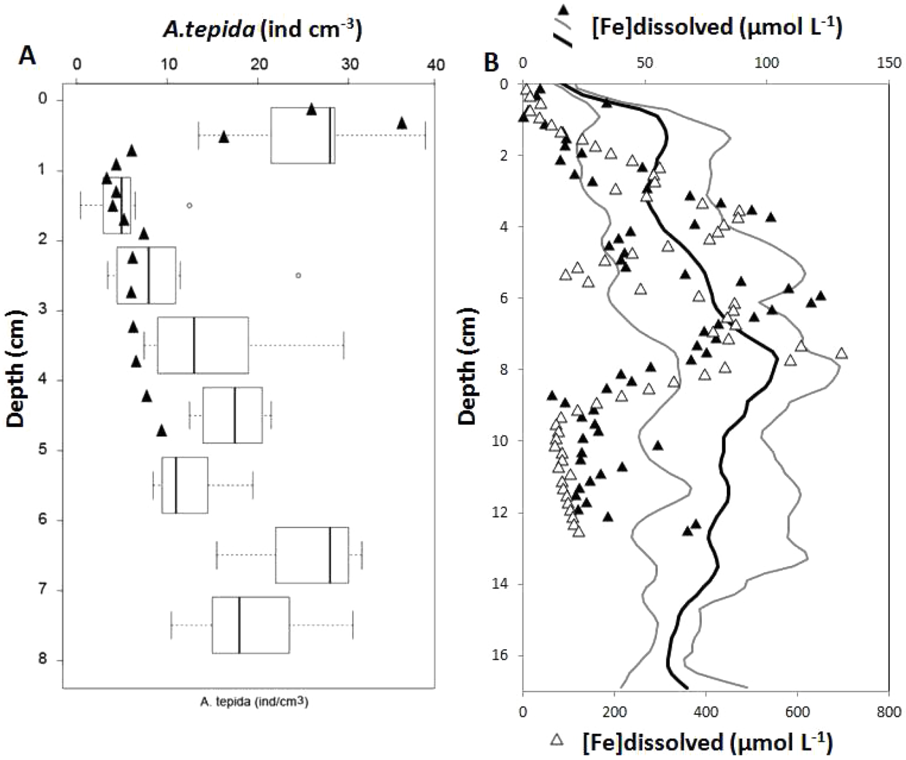

Figure 8. (a) Vertical comparison between *A. tepida* density from the core (full triangle) and the "jaw device" sampling (boxplots). Bars are first and third quartiles for the box length and whiskers are below 1.5 interquartile ranges for 8 replicates (one row), open circle are outliers. **(b)** Vertical comparison between dissolved iron concentration from replicates of the DET-1D (full and open triangles) and the DET-1D equivalent mean and extrema. Note that open triangles are represented in a different scale.

Title Page
Abstract
Introduction
Conclusions
References
Tables
Figures
◀I
I▶
◀
▶
Back
Close
Full Screen / Esc
Printer-friendly Version
Interactive Discussion

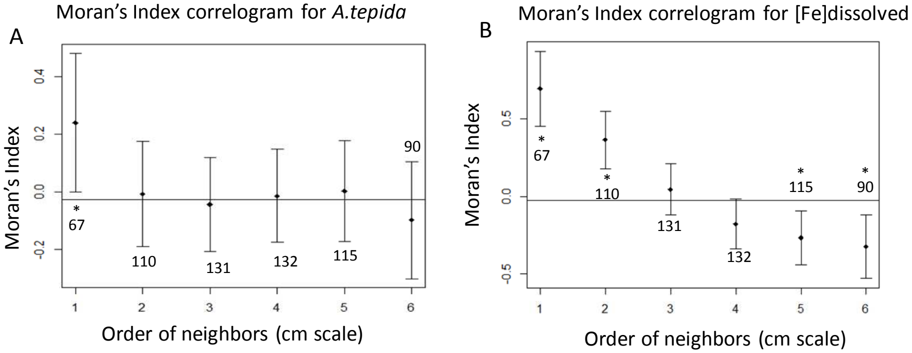

Figure 9. Moran's Index Correlograms for 3 to 8 cm depth: **(a)** Moran's Index correlogram for *A. tepida* at a resolution of 1 cm. **(b)** Moran's Index correlogram for [Fe] dissolved at a resolution of 1 cm. * shows significant difference with zero, error bars are twice the standard deviation, the numbers are the number of pairs for each order of neighbors.

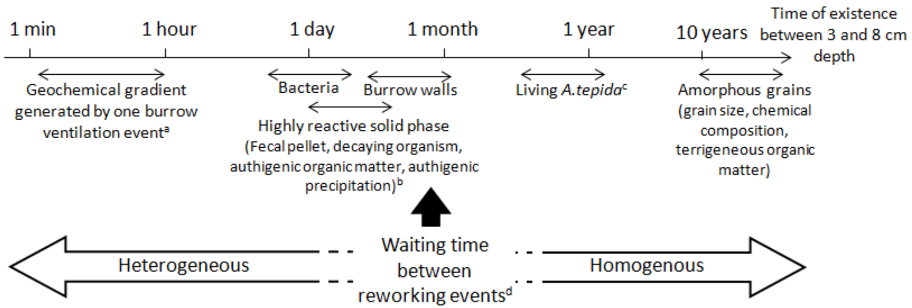

Figure 10. Model of bioturbation impact on spatial heterogeneity, adapted from Meysman et al. (2008). [a] from Fenchel (1996); Wenzhofer and Glud (2004), [b] from Alldredge and Cohen (1987); Zhu et al. (2006), [c] from Heinz and Geslin (2012); Nardelli et al. (2014), [d] from Meysman et al. (2003).

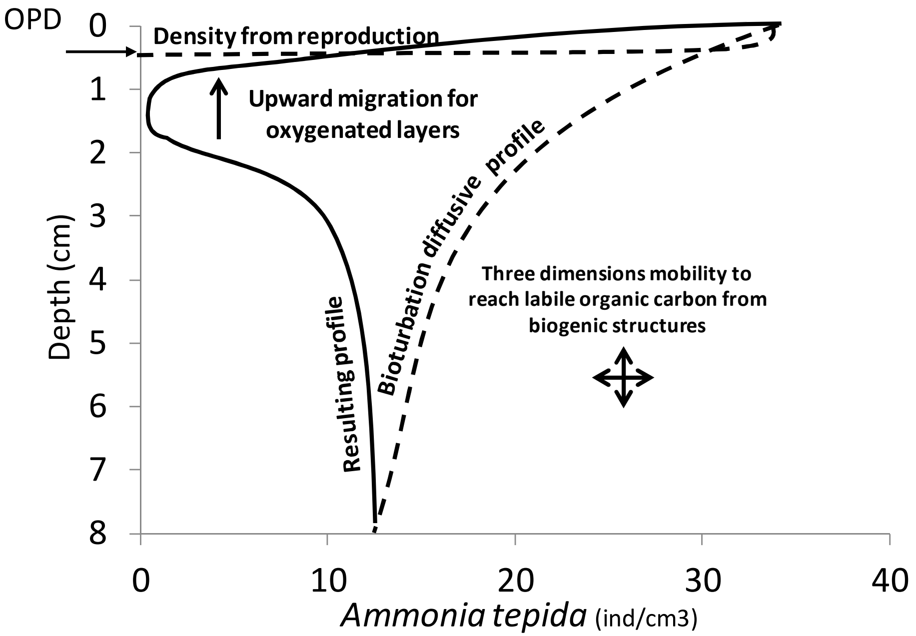

Figure 11. Proposition of mechanisms to explain *A. tepida* density profile (OPD = Oxygen penetration depth).